



## Mathematical modeling of the drug release from an ensemble of coated pellets

Journal:	<i>British Journal of Pharmacology</i>
Manuscript ID	2016-BJP-1037-RP.R2
Manuscript Type:	Research Paper
Date Submitted by the Author:	n/a
Complete List of Authors:	Caccavo, Diego; Dep. Industrial Engineering Lamberti, Gaetano; Dep. Industrial Engineering Cafaro, Maria Margherita; Dep. Industrial Engineering Barba, Anna Angela; University of Salerno Kazlauske, Jurgita; AstraZeneca Larsson, Anette; Chalmers University of Technology
Major area of pharmacology:	Translational Pharmacology
Cross-cutting area:	Drug delivery
Additional area(s):	Mathematical modeling

SCHOLARONE™  
Manuscripts

We would like to thank the Reviewers and the Editor for their constructive comments. In the following, the criticisms raised by the reviewers (in black) and our answer (in blue) are reported. The required changes in the manuscript text have been done in red.

We wish to express once again our appreciation for the in-depth comments, suggestions, and corrections of the reviewers, which have greatly improved the manuscript.

## Editor

Comments to the Author

Authors have addressed all comments adequately.

## Reviewer: 1

Comments to the Author

The authors properly accounted for all my issues.

## Reviewer: 2

Comments to the Author

The authors paid careful attention to the many comments of the previous reviewers. The manuscript is greatly strengthened in clarity and readability.

I have **no major concerns** remaining after the revision. The response to Reviewer 2 major concern #12 was adequately answered in the response to reviewers, but it is still a bit unclear in the text. The reviewer recommends including a statement somewhere that the six classes of inert core SD are not the same 10 classes defined for film thickness SD in Table 3.

The following sentence has been added in the section “4. Discussion and Conclusions”:

“In modeling the inert core SD (Figure 8) six classes were used, different in the inert core radius, reported in eq. (19). In modeling the film thickness SD (Figure 9 and Table 3) ten classes were used, which differ in the film thickness dimensions (reported in Table 3).”

The following list of **minor issues** and recommendations should be considered if accepted:

1. Page 1 final line: “demonstrating to be” should be “demonstrating its use as”  
Done.
2. Page 2 Section 1.1 line 1: patient compliance or compliance among patients  
Done.
3. Page 2 Section 1.1 line 3: keep only the red text and remove the preceding “particulate systems” and the parenthesis.  
Done.
4. Page 2 Section 1.2 lines 1-2: same comment as 3.  
Done.
5. Page 2 section 1.2 lines 17-18: Put a period after (2011) and start a new sentence with “However,”  
Done.
6. Page 2 section 1.2 line 20: considered

Done.

7. Page 4 final line: recommended to break the long sentence into two. “work. As” (remove the conjunction since)

Done.

8. Page 6 Lines 1-2: Put a period after (2013) and start a new sentence with “Therefore,”

Done.

9. Page 6 just before eq. (3), “according to eq. (5) and (7), respectively.”

Done.

10. Page 9 Table 2 caption: “value. It is”

Done.

11. Page 9 Table 2: instead of ODE, the heading would be clearer as “ODE eq. number”

Done.

12. Page 9 subsection on heterogeneous systems line 1: “shown”

Done.

13. Page 10 line 3: “ODEs given by eq. (1), ...for each of the six classes

Done.

14. Starting on page 10 several equations have parenthesis around them as in (eq. (1)). The comma offset notation, eq. (1), was used earlier in the text.

The comma offset notation has been adopted for all the cited equations.

15. Page 11 section 3.1.1 remove comma before and

Done.

16. Page 12 Figure 3 caption: size distribution

Done.

17. Page 13 section 3.2 lines 3-4: “considering unitary the covering efficiency”, is awkwardly worded. Perhaps something like “considering a uniform covering efficiency of 100%”

Done.

18. Page 15 Homogeneous system line 1: add “and” between 1-12 and 16-18

Done.

19. Page 15 Heterogeneous system line 1: add “and” between 16, and 19-25

Done.

20. Page 15 second line from bottom: “polymeric layers”

Done.

21. Page 16 Figure 8 caption: described

Done.

22. Page 16 Relevance of SD... line 1 “16, and 23-32”

Done.

23. Page 18 third line from bottom: The sentence in red along with the “In literature” phrase doesn’t make sense. The next sentence should also be polished and perhaps broken into two sentences. The use of “this” introduces ambiguity when it could refer to different topics each time.

Both the sentences have been reformulated in:

“To reproduce the experimental sigmoidal drug release results from ensembles of pellets drug diffusion coefficients function of the dissolution time could be used (i.e. Marucci et al. (2013)), based on the assumption that morphological changes of the polymeric film modify the diffusive process.”

# Mathematical modeling of the drug release from an ensemble of coated pellets

Diego CACCAVO<sup>1</sup>, Gaetano LAMBERTI<sup>1,\*</sup>, Maria Margherita CAFARO<sup>1</sup>, Anna Angela BARBA<sup>2</sup>

Jurgita KAZLAUSKE<sup>3</sup>, Anette LARSSON<sup>4,5</sup>

<sup>1</sup>Department of Industrial Engineering, University of Salerno, 84084 Fisciano (SA), Italy

<sup>2</sup> Department of Pharmacy, University of Salerno, 84084 Fisciano (SA), Italy

<sup>3</sup> AstraZeneca R&S, Mölndal, Sweden

<sup>4</sup> Pharmaceutical Technology, Department of Chemical Engineering, Chalmers University of Technology

<sup>5</sup> SuMo BIOMATERIALS, A VINNOVA VINN Excellence Center at Chalmers University of Technology

\* Tel +39 089 964077; glamberti@unisa.it

## Abstract

**Background and Purpose.** Coated pellets are widely used as oral drug delivery systems, being highly accepted by patients and with several advantages with respect to single unit devices. The understanding of their behavior is therefore needed to improve the formulation effectiveness and to reduce the production costs. In spite of such an importance, not many mathematical modeling attempts have been made, mostly due to the complexities arising from the system polydispersity (non homogeneous multiple-unit particulate systems), which has been scarcely investigated with the aid of mechanistic models.

**Experimental approach.** In this work a mechanistic mathematical model able to describe the single pellet behavior in terms of hydration, drug dissolution, diffusion and release, and particle size change was developed. This model was then extended to describe and predict the behavior of mono- and poly-disperse ensembles of pellets.

**Key Results.** In particular the polydispersity arising from the inert core size distribution was proved to have a minimal effect on the drug release profile, whereas the size distribution of the polymeric film thickness showed to be the key parameter determining the drug release.

**Conclusions and Implications.** The developed mechanistic model, capable of considering the polydispersity of the system, was able to predict the release kinetics from ensembles of pellets and to highlight the key parameters to control in the production of pellets-based drug delivery systems, demonstrating *its use as* a powerful predictive tool.

## Abbreviations

Initial conditions,	ICs
Hydroxypropyl methylcellulose,	HPMC
Ordinary differential equations,	ODEs
Particle size distribution,	PSD
Size distribution,	SD

## 1. Introduction

### 1.1 Generalities

The oral route for drug administration is one of the most used due to the high **patient compliance** and the high mass-exchange surface available in the gastro-intestinal tract. Many oral pharmaceuticals are prepared as **multiple-unit particulate systems** since they present several advantages over the single unit device – i.e. reduction of the local drug concentration with the resulting reduction of the gastric irritation phenomenon (Grassi, Grassi, Lapasin & Colombo, 2006), fast gastric emptying and long residence time in the intestine (Abrahamsson et al., 1996). Among the particulate systems, often the coated pellets are the most used to obtain controlled drug release. The insoluble polymer layer covers the pellets, tunes the drug release, masks undesirable tastes of drugs, and improves the device stability by protecting the inner part from the external environment (Siepmann, Siepmann, Walther, MacRae & Bodmeier, 2008).

### 1.2 State of the art

Modeling ensembles of coated pellets is a complicated task due to the polydisperse character of **non homogeneous multiple-unit particulate systems**, and not many modeling attempts have been made. Dappert and Thies (1978) with their statistical based model, followed by Gross, Hoffman, Donbrow and Benita (1986) and Donbrow, Hoffman and Benita (1988), have demonstrated that the cumulative release of a poly-disperse system does not characterize the basic release mechanism, and they clearly showed that the form of the release profile from a single pellet differs from the release profile of an ensemble. These authors have also demonstrated that cumulative amount of drug release pertaining to the ensemble of polydisperse particles can be deduced from the cumulative release of each particle class. A particle class defines a dimensional range in which a certain number or mass (numerical or mass distribution) of particles can be individuated. The particles falling in a class can be described with the average dimension of the class (i.e. mean diameter). In their model the mutual interaction between particle classes was neglected. Grassi, Colombo and Lapasin (2000) utilized a mechanistic model to analyze the drug release from an ensemble of swellable crosslinked polymer particles with a known initial particle size distribution (PSD). Borgquist, Zackrisson, Nilsson and Axelsson (2002) and Borgquist, Nevsten, Nilsson, Wallenberg and Axelsson (2004) developed a mechanistic model to describe drug release from ensembles of coated pellets but neglected the interaction between the dimensional classes of pellets. Other attempts have been done in the years, some of them reported in Kaunisto, Marucci, Borgquist and Axelsson (2011). However, most of these mechanistic works neglected the interaction between ensembles of particles with the same size, namely 'classes', i.e the drug released from one class does not influence the drug release from the other classes (perfect sink condition), and considered the polydispersity generated only by difference in internal drug core radius, disregarding variation of the polymeric film thickness. To our knowledge, a mathematical model able to describe the mass fraction evolution of all the species along with the system deformation, accounting for the size distribution of the different layers has never been proposed in the case of coated pellets.

### 1.3 Aims

There are two aims of this work. The first aim is to develop a mechanistic (or first principles) mathematical model able to describe the drug dissolution and release, as well as the system deformation, from a single pellet made of an inert core, a drug and a polymeric layer. The second aim is to describe the behavior of an ensemble of mono- and poly-disperse pellets through the extension of the single pellet model. The polydispersity will be considered as potentially arising from the size distribution of each pellet layer.

## 2. Materials and methods

The materials and methods used to produce the coated pellets and test the drug release are described in detail in Kazlauske et al. (submitted). For sake of completeness, in paragraphs 2.1-2.4, these steps will be briefly reported.

### 2.1 Materials

The inert cores of pellets were made of microcrystalline cellulose spheres (Cellets® 500, Syntapharm GmbH, Germany). Anhydrous theophylline, our model drug, was bought from Sigma-Aldrich (USA). HydroxyPropyl MethylCellulose (HPMC) 5 cP, used as plasticizer within the drug layer, was a gift from Dow Chemical - USA. The coating was made of Surelease®E-7-19020, aqueous ethyl cellulose dispersion (24.7% w/w, Colorcon, USA). Sodium phosphate monobasic monohydrate and disodium phosphate for the preparation of buffered release medium were bought from Sigma-Aldrich (USA).

### 2.2. Production of coated pellets

The pellets analyzed in this work were produced by the solution/suspension layering technique, which requires a starter core (nucleation seed) to promote the process. The coating was performed in a fluid bed coater equipped with a Wurster column (Gandalf 0, AstraZeneca, Sweden) in two steps. In the first step the Cellets® spheres (starter core) were coated with a Theophylline:HPMC solution (90:10 w/w) to produce the drug layer. In the second step the drug covered pellets were coated with the aqueous ethyl cellulose dispersion to obtain the polymeric film layer. The operating conditions are reported in Kazlauske et al. (submitted) and briefly summarized in the following. Theophylline:HPMC (weight ratio 90:10) solution was sprayed on microcrystalline cores. These coated pellets were sprayed with an ethyl cellulose layers using Surelease (15% w/w) at an inlet temperature of 45°C and cured at 50°C for 24 h in an oven. The operative conditions were chosen to produce a theoretical drug layer thickness of 12 µm and theoretical polymeric film thickness of 20, 30 and 60 µm, respectively ( $f_t20$ ,  $f_t30$ ,  $f_t60$ ). The theoretical film thickness in microns is denoted as  $f_t x$  where  $x$  is the thickness value.

### 2.3 Drug release

Drug release from an ensemble of pellets, 500 mg, was analyzed in an USP II apparatus (Varian 705DS, Varian Inc., USA) at 37°C, 100 rpm in 1 L of phosphate buffer (pH 6.8). Samples of 3 mL were automatically collected (8000 Dissolution sampling station, Agilent Technologies, USA) and analyzed by a spectrophotometer (Cary 60 UV-Vis, Agilent Technologies, USA) at 272 nm calculating the drug concentration in the medium and the drug release profiles.

### 2.4 Surelease film properties

#### 2.4.1 Diffusivity measurements

The measurement of the water and Theophylline diffusivity within the polymeric film were performed in a diffusion cell with a donor and an acceptor compartment separated by a square piece (1.5×1.5 cm) of the polymeric film. The amount of tritium-labelled water and Theophylline passing from the donor to the acceptor compartment were monitored respectively with a scintillation counter (TriCarb 2810TR, PerkinElmer, USA) and a spectrophotometer (Cary 60 UV-Vis, Agilent Technologies, USA) at 272 nm.

#### 2.4.2 Swelling of Surelease free film

Three free films of Surelease (Kazlauske et al., submitted) with a weight of 36.1±4.2 mg and a thickness of 141.8±9.6 µm were put in 100 ml of distilled water at 37°C and hydrated. The films were withdrawn at

several times, in the interval 0-80 h, and weighed to determine the weight variation attributed to the amount of water absorbed.

## 2.5 Particle size distribution of Cellets

The PSD of Cellets® 500 was estimated with a laser scattering granulometer (Mastersizer 3000, Malvern), equipped with the Hydro EV apparatus to create wet dispersions. Distilled water was used as dispersant.

## 2.6 Polymer and drug thickness layers

The thickness of the polymeric layer was measured analyzing cross sections of the pellets. The procedure to obtain pellets cross sections for the SEM images (Figure 4/A) was described in Kazlauske et al. (submitted): the pellets were immobilized in paraffin wax and cut with a cryostat-microtome (Electronic cryostat Cryotome E, Thermo Electron Corporation, Runcorn). Cross sections of pellets analyzed with the optical microscope (Leica DMLP, USA), reported in Figure 4/B, were obtained by immobilizing the pellets in polyester resin (Solver Italia, Italy) and cutting with a semi-automated rotary microtome (Leica RM2245).

## 2.7. Modeling

### 2.7.1 Phenomenology

A pellet is depicted schematically in Figure 1. The phenomenological hypotheses are the following:

- the water from the external environment ( $\Omega_D$ ) diffuses into the pellet through the coating ( $\Omega_C$ ), which swells ( $R_C(t)$  increases), causing the hydration of the internal parts;
- the drug and the HPMC dissolve, with the same kinetics, from the solid layer ( $\Omega_A$ :  $R_A(t)$  decreases) into the liquid layer ( $\Omega_B$ :  $R_B(t)$  increases);
- the dissolved drug from the liquid layer diffuses through the polymeric coating ( $\Omega_C$ ) and accumulate in the external environment ( $\Omega_D$ );
- meanwhile the liquid layer continues to increase in volume due to the water inlet from  $\Omega_C$  ( $R_B(t)$  increases), causing the stretching of the polymeric coating ( $\Omega_C$  ( $R_C(t) - R_B(t)$  decreases) due to its limited swelling capacity.

Although it has been experimentally seen that the Cellets® swell in PBS increasing the radius by about 10%, in this model this phenomenon is disregarded, because the water reaches the core only once the drug layer has been completely dissolved and almost completely released. The inclusion of this effect, even if it is not difficult to be implemented, would require the definition of other parameters – like the water diffusivity and the MCC/water equilibrium constant – that are not easily available and would add little in terms of description of real behavior. Osmotic pressure driven release, which manifests in case of polymeric film pores/cracks, is not considered in this work. As experimentally proven by (Kazlauske et al., submitted), this phenomena in this system is absent.

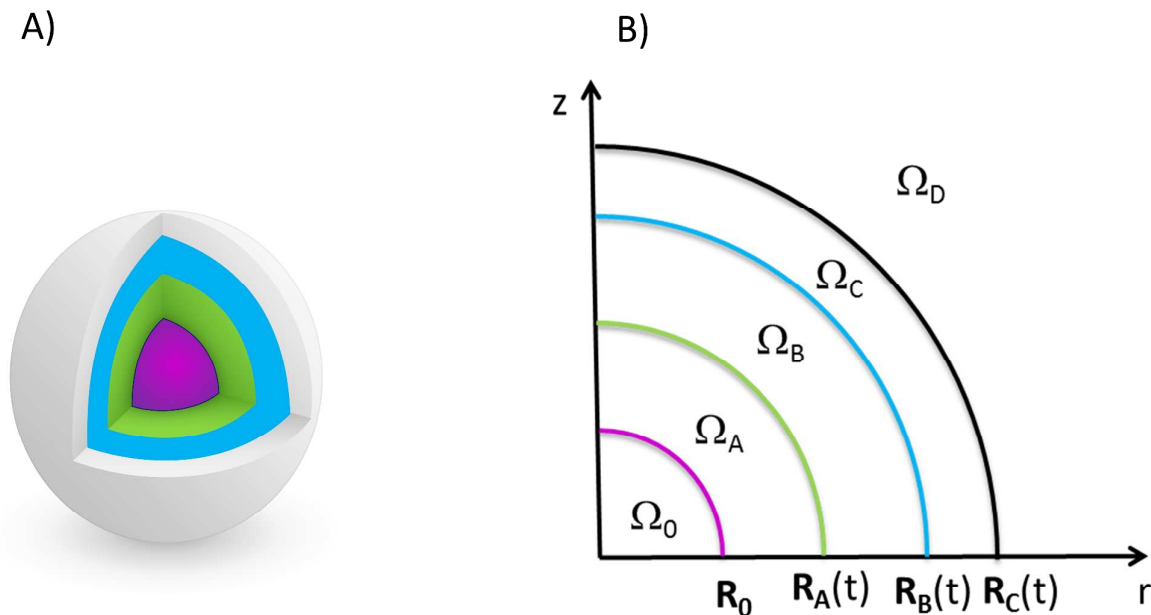


Figure 1. 3D representation of a pellet A) with its 2D axisymmetric schematization B).  $\Omega_0$  represents the inert core (Cellets®) with fixed radius  $R_0$ .  $\Omega_A$  represents the solid drug layer (drug and HPMC) with the time-dependent outer radius  $R_A(t)$ .  $\Omega_B$  represents the dissolved drug layer (drug, HPMC, and water) with time-dependent outer radius  $R_B(t)$ .  $\Omega_C$  represents the polymeric film layer (Surelease, drug, and water) with the time-dependent outer radius  $R_C(t)$ .  $\Omega_D$  represents the dissolution medium (drug and water) in which the pellet is immersed.

### 2.7.2 Single pellet modeling

The system is described with a lumped approach, so that each domain has a homogeneous value of mass fraction of each species. In each domain the mass balances for the N-1 species, where N is the total number of species, as well as the total mass balance are written and solved for the species mass fractions and the domain dimensions, respectively. In the following the species are indicated with the subscripts 1 (water), 2 (Theophylline), 3 (HPMC) and 4 (Surelease). The domain at which the variable is referring to is indicated with a superscript letter. The model parameters, discussed in the following, are reported in Table 1.

#### Domain $\Omega_A$

The domain  $\Omega_A$  represents the solid Theophylline/HPMC layer. In this domain the mass fraction of drug and polymer are constant and equal to the initial value:  $\omega_2^A = \omega_{20}^A = 0.9$  and  $\omega_3^A = \omega_{30}^A = 0.1$ . Since the mass fractions are fixed, the domain density ( $\rho^A$ ) is constant, and the mass balance on a species is sufficient to describe the system deformation ( $R_A(t)$ ). The mass balance on the dissolving drug can be written using the Noyes and Whitney (1897) equation:

$$\frac{dm_2^A}{dt} = \frac{d(\rho^A \omega_{20}^A \Omega_A)}{dt} = -4\pi R_A^2 k_{\text{diss}} \rho^B (\omega_{2,\text{sat}}^B - \omega_2^B) \quad (1)$$

$$R_A(t=0) = R_{A0}$$

$$\frac{1}{\rho^A} = \left( \frac{\omega_{20}^A}{\rho_{20}} + \frac{\omega_{30}^A}{\rho_{30}} \right) = \text{constant} \quad (2)$$

where  $k_{\text{diss}}$  is the dissolution rate constant, which describes the mass transfer rate from the solid layer into the liquid layer. Following Marucci et al. (2013), the dissolution rate can be estimated from the Sherwood correlation for a sphere by  $Sh = 2 + 0.6Re^{1/2}Sc^{1/3}$  (Bird, Stewart & Lightfoot, 2007) considering that the

Mathematical modeling of the drug release  
from an ensemble of coated pellets

D. CACCAVO, G. LAMBERTI, M.M. CAFARO, A.A. BARBA  
J. KAZLAUSKE, A. LARSSON

product  $Re^{1/2}Sc^{1/3}$  is very small due to the internal stagnant conditions (Manca & Rovaglio, 2003). Therefore,  $Sh = 2$  and thus  $k_{diss} = D_2^B/R_A$ . The parameter  $D_2^B$  is the Theophylline diffusivity in the domain  $\Omega_B$ , which is a water rich solution with low percentage of HPMC and Theophylline, a situation analogous to the fully swollen matrix of Caccavo, Cascone, Lamberti and Barba (2015), from which the value of the  $D_2^B$  was taken ( $1.5 \times 10^{-10}$  [m<sup>2</sup>/s]). The mass fraction  $\omega_{2,sat}^B = 0.0115$  represents the Theophylline saturation mass fraction at the solid-liquid interface (calculated from the solubility in water at 37°C: 11.6 g/l (Serajuddin & Jarowski, 1985)).

#### Domain $\Omega_B$

The domain  $\Omega_B$  represents the internal liquid layer made of a water solution of HPMC and Theophylline. In this layer the drug enters from  $\Omega_A$  (due to the solid layer dissolution) and leaves diffusing toward  $\Omega_C$  (first and second term at right hand side of eq. (3)). The HPMC, eq. (4), can only enter in this domain, following the dissolution of the Theophylline, but cannot be released (the diffusivity of the HPMC in the Surelease layer goes to zero). Water can enter into this region from the polymer coating, eq. (6), and the total mass of the system and its density vary according eq. (5) and (7), respectively.

$$\frac{dm_2^B}{dt} = \frac{d(\rho^B \omega_2^B \Omega_B)}{dt} = 4\pi R_A^2 k_{diss} \rho^B (\omega_{2,sat}^B - \omega_2^B) - 4\pi R_B^2 K_2^{BC} (\rho^B \omega_2^B - \rho^C \omega_2^C) = \dot{m}_2^B \quad (3)$$

$$\omega_2^B(t=0) = \omega_{20}^B$$

$$\frac{dm_3^B}{dt} = -\frac{dm_3^A}{dt} = \frac{d(\rho^B \omega_3^B \Omega_B)}{dt} = 4\pi R_A^2 \frac{\omega_{30}^A}{\omega_{20}^A} k_{diss} \rho^B (\omega_{2,sat}^B - \omega_2^B) = \dot{m}_3^B \quad (4)$$

$$\omega_3^B(t=0) = \omega_{30}^B$$

$$\frac{dm^B}{dt} = \frac{d(\rho^B \Omega_B)}{dt} = \dot{m}_1^B + \dot{m}_2^B + \dot{m}_3^B \quad (5)$$

$$R_B(t=0) = R_{B0}$$

$$\dot{m}_1^B = 4\pi R_B^2 K_1^{BC} (m_1^{BC} \rho^C \omega_1^C - \rho^B \omega_1^B) \quad (6)$$

$$\frac{1}{\rho^B} = \left( \frac{1 - \omega_2^B - \omega_3^B}{\rho_{10}} + \frac{\omega_2^B}{\rho_{20}} + \frac{\omega_3^B}{\rho_{30}} \right) \quad (7)$$

The transport parameter  $K_2^{BC}$  is the overall time dependent Theophylline mass transport coefficient between  $\Omega_B$  and  $\Omega_C$ , defined in Table 1, which is a function of the Theophylline diffusivities in both the domains:  $D_2^B$  (from Caccavo, Cascone, Lamberti and Barba (2015)) and  $D_2^C$  (from the experimental results of Kazlauske et al. (submitted)). Similarly  $K_1^{BC}$  is the overall water mass transport coefficient between  $\Omega_B$  and  $\Omega_C$ , defined in Table 1, which is a time dependent function related to the parameters  $D_1^B$  (from Caccavo, Cascone, Lamberti and Barba (2015)),  $D_1^C$  (from Kazlauske et al. (submitted)) and to the equilibrium constant  $m_1^{BC}$ . The equilibrium constant  $m_1^{BC}$  relates the water mass fraction in  $\Omega_C$  to its equilibrium counterpart in  $\Omega_B$ :  $\omega_{1,eq}^B = m_1^{BC} \omega_{1,eq}^C$ . Knowing that  $\omega_{1,eq}^C \approx 0.2$  from the Surelease free film swelling tests and considering that  $\omega_{1,eq}^B \rightarrow 1$  ( $\sim 0.99$ ), results in that  $m_1^{BC} \rightarrow 5$  (being  $\omega_{1,eq}^B = m_1^{BC} \omega_{1,eq}^C$  and then  $m_1^{BC} = \omega_{1,eq}^B / \omega_{1,eq}^C \sim 4.95$ ). This will allow the inlet of water in the domain  $\Omega_B$  until its mass fraction reaches the 99%, which is the equilibrium value. The domain  $\Omega_B$  at time zero, physically nonexistent, is mathematically represented by a very thin layer ( $3 \times 10^{-9}$  [ $\mu\text{m}$ ]) made of pure water, for numerical reasons, to avoid singularities.

*Domain  $\Omega_C$* 

This domain represents the polymer coating through which Theophylline and water can diffuse. In particular the Theophylline diffuses from the inner layer, the liquid layer  $\Omega_B$ , and leaves the domain diffusing toward  $\Omega_D$  (first and second term at right hand side of eq. (8)). The Surelease in this case does not enter or leave the system, therefore its mass is constant, eq. (9), but its mass fraction is not constant. Water can enter or leave this domain from both the dissolution medium ( $\Omega_D$ ) and the liquid layer ( $\Omega_B$ ), eq. (11). The total mass of the system and its density vary according to eq. (10) and (12) respectively.

$$\frac{dm_2^C}{dt} = \frac{d(\rho^C \omega_2^C \Omega_C)}{dt} = 4\pi R_B^2 K_2^{BC} (\rho^B \omega_2^B - \rho^C \omega_2^C) - 4\pi R_C^2 K_2^{CD} (\rho^C \omega_2^C - \rho^D \omega_2^D) = \dot{m}_2^C \quad (8)$$

$$\omega_2^C(t=0) = \omega_{20}^C$$

$$\frac{dm_4^C}{dt} = \frac{d(\rho^C \omega_4^C \Omega_C)}{dt} = 0 = \dot{m}_4^C \quad (9)$$

$$\omega_4^C(t=0) = \omega_{40}^C$$

$$\frac{dm^C}{dt} = \frac{d(\rho^C \Omega_C)}{dt} = \dot{m}_1^C + \dot{m}_2^C + \dot{m}_4^C \quad (10)$$

$$R_C(t=0) = R_{C0}$$

$$\dot{m}_1^C = 4\pi R_C^2 K_1^{CD} (m_1^{CD} \rho^D \omega_1^D - \rho^C \omega_1^C) - 4\pi R_B^2 K_1^{BC} (m_1^{BC} \rho^C \omega_1^C - \rho^B \omega_1^B) \quad (11)$$

$$\frac{1}{\rho^C} = \left( \frac{1 - \omega_2^C - \omega_4^C}{\rho_{10}} + \frac{\omega_2^C}{\rho_{20}} + \frac{\omega_4^C}{\rho_{40}} \right) \quad (12)$$

Likewise  $K_2^{BC}$ , the transport parameter  $K_2^{CD}$  is the overall Theophylline mass transport coefficient between  $\Omega_C$  and  $\Omega_D$ , defined in Table 1, which is a time dependent function related to the parameters  $D_2^C$  and  $D_2^D$ , this last being the diffusion coefficient of the Theophylline in water at 37°C ( $8.21 \times 10^{-10}$  [m<sup>2</sup>/s] (Grassi, Colombo & Lapasin, 2001)).  $K_1^{CD}$  is the overall water mass transport coefficient between  $\Omega_C$  and  $\Omega_D$ , defined in Table 1, which is a time dependent function related to the parameters  $D_1^C$ ,  $D_1^D$  and  $m_1^{CD}$ .  $D_1^D$  is the self-diffusion coefficient of water in water at 37°C ( $3 \times 10^{-9}$  [m<sup>2</sup>/s] (Holz, Heil & Sacco, 2000)). The equilibrium constant  $m_1^{CD}$  relates the water mass fraction in  $\Omega_D$  to its equilibrium counterpart in  $\Omega_C$ :  $\omega_{1,eq}^C = m_1^{CD} \omega_{1,eq}^D$ . Knowing from the Surelease free film swelling tests that  $\omega_{1,eq}^C \approx 0.2$  and considering that  $\omega_{1,eq}^D \approx 1$  results in  $m_1^{CD} = 0.2$ .

*Domain  $\Omega_D$* 

The domain  $\Omega_D$  represents the dissolution medium. Theophylline can reach this domain diffusing through the polymer coating, eq. (13). The total mass of this domain, eq. (14), can vary due to water outlet, described by eq. (15), and drug inlet.

$$\frac{dm_2^D}{dt} = \frac{d(\rho^D \omega_2^D \Omega_D)}{dt} = 4\pi R_C^2 K_2^{CD} (\rho^C \omega_2^C - \rho^D \omega_2^D) = \dot{m}_2^D \quad (13)$$

$$\omega_2^D(t=0) = \omega_{20}^D$$

$$\frac{dm^D}{dt} = \frac{d(\rho^D \Omega_D)}{dt} = \dot{m}_2^D - \dot{m}_1^D \quad (14)$$

$$\Omega_D(t=0) = \Omega_{D0}$$

Mathematical modeling of the drug release  
from an ensemble of coated pellets

D. CACCAVO, G. LAMBERTI, M.M. CAFARO, A.A. BARBA  
J. KAZLAUSKE, A. LARSSON

$$\dot{m}_1^D = 4\pi R_C^2 K_1^{CD} (m_1^{CD} \rho^D \omega_1^D - \rho^C \omega_1^C) \quad (15)$$

$$\frac{1}{\rho^D} = \left( \frac{1 - \omega_2^D}{\rho_{10}} + \frac{\omega_2^D}{\rho_{20}} \right) \quad (16)$$

Despite the mass variation of the dissolution medium being negligible in normal dissolution tests where  $\Omega_D \gg (\Omega_A + \Omega_B + \Omega_C)$ , this might not be negligible in single pellet release tests.

Table 1. Model parameters.

Independent Parameters	Value	Description
$D_1^B$	$2.2 \times 10^{-9}$ [m <sup>2</sup> /s] (Caccavo, Cascone, Lamberti & Barba, 2015)	Water diffusivity in the dissolved drug layer ( $\Omega_B$ )
$D_2^B$	$1.5 \times 10^{-10}$ [m <sup>2</sup> /s] (Caccavo, Cascone, Lamberti & Barba, 2015)	Drug diffusivity in the dissolved drug layer ( $\Omega_B$ )
$D_1^C$	$1.99 \times 10^{-12}$ [m <sup>2</sup> /s] (Kazlauske et al., submitted)	Water diffusivity in the polymeric film ( $\Omega_C$ )
$D_2^C$	$3.1 \times 10^{-13}$ [m <sup>2</sup> /s] (Kazlauske et al., submitted)	Drug diffusivity in the polymeric film ( $\Omega_C$ )
$D_1^D$	$3 \times 10^{-9}$ [m <sup>2</sup> /s] (Holz, Heil & Sacco, 2000)	Water diffusivity in the dissolution medium ( $\Omega_D$ )
$D_2^D$	$8.21 \times 10^{-10}$ [m <sup>2</sup> /s] (Grassi, Colombo & Lapasin, 2001)	Drug diffusivity in the dissolution medium ( $\Omega_D$ )
$\omega_{2,sat}^B$	0.0115 [-] (Serajuddin & Jarowski, 1985)	Theophylline saturation mass fraction in water
$m_1^{BC}$	4.95 [-] (from experiment)	Water equilibrium constant: relates the water mass fraction in $\Omega_C$ to its equilibrium counterpart in $\Omega_B$
$m_1^{CD}$	0.2 [-] (from experiment)	Water equilibrium constant: relates the water mass fraction in $\Omega_D$ to its equilibrium counterpart in $\Omega_C$
$\rho_{10}$	1000 [kg/m <sup>3</sup> ] (Caccavo, Cascone, Lamberti & Barba, 2015)	Pure water density
$\rho_{20}$	1200 [kg/m <sup>3</sup> ] (Caccavo, Cascone, Lamberti & Barba, 2015)	Pure Theophylline density
$\rho_{30}$	1200 [kg/m <sup>3</sup> ] (Caccavo, Cascone, Lamberti & Barba, 2015)	Pure HPMC density
$\rho_{40}$	1200 [kg/m <sup>3</sup> ]	Pure Surelease density
Dependent Parameters	Expression	
$k_{diss}$	$D_2^B/R_A$	Theophylline dissolution rate constant
$K_1^{BC}$	$(1/k_1^B + m_1^{BC}/k_1^C)^{-1}$	Overall water mass transport coefficient between $\Omega_B$ and $\Omega_C$
$K_2^{BC}$	$(1/k_2^B + 1/k_2^C)^{-1}$	Overall Theophylline mass transport coefficient between $\Omega_B$ and $\Omega_C$
$k_1^B$	$D_1^B/(R_B - R_A)$	Water mass transport coefficient between $\Omega_B$
$k_2^B$	$D_2^B/(R_B - R_A)$	Theophylline mass transport coefficient between $\Omega_B$
$K_1^{CD}$	$(1/k_1^C + m_1^{CD}/k_1^D)^{-1}$	Overall water mass transport coefficient between $\Omega_C$ and $\Omega_D$
$K_2^{CD}$	$(1/k_2^C + 1/k_2^D)^{-1}$	Overall Theophylline mass transport coefficient between $\Omega_C$ and $\Omega_D$
$k_1^C$	$D_1^C/(R_C - R_B)$	Water mass transport coefficient between $\Omega_C$

Mathematical modeling of the drug release  
from an ensemble of coated pellets

D. CACCAVO, G. LAMBERTI, M.M. CAFARO, A.A. BARBA  
J. KAZLAUSKE, A. LARSSON

$k_2^C$	$D_2^C/(R_C - R_B)$	Theophylline mass transport coefficient between $\Omega_C$
$k_1^D$	$D_1^D/R_C$	Water mass transport coefficient between $\Omega_D$
$k_2^D$	$D_2^D/R_C$	Theophylline mass transport coefficient between $\Omega_D$

**Table 2.** Single pellet model variables with the respective ODE eq. number and the initial value of the variable. The radii with the asterisks are theoretical values. It is assumed that all the Surelease sprayed goes onto the pellets.

Variable	ODE	Initial value
$R_A$	1	$306 - 3 \times 10^{-9}$ [ $\mu\text{m}$ ]
$R_B$	5	306 [ $\mu\text{m}$ ]
$R_C$	10	326* or 336* or 366* [ $\mu\text{m}$ ]
$\omega_2^B$	3	0
$\omega_3^B$	4	0
$\omega_2^C$	8	0
$\omega_4^C$	9	1
$\omega_2^D$	13	0
$\Omega_D$	14	1 [L]

### 2.7.3 Ensemble of pellets modeling

#### Homogeneous system

When modeling the drug release from an ensemble of pellets, the first conceivable approach is to consider the whole dose made of perfectly equal pellets (monodisperse system). This assumption requires a minimum variation of the equations presented in the section 2.7.2, in particular the mass balances in the domain  $\Omega_D$ , eq. (13) and (14), become:

$$\frac{dm_2^D}{dt} = \frac{d(\rho^D \omega_2^D \Omega_D)}{dt} = N_P 4\pi R_C^2 K_2^{CD} (\rho^C \omega_2^C - \rho^D \omega_2^D) = \dot{m}_2^D \quad (17)$$

$$\omega_2^D(t=0) = \omega_{20}^D$$

$$\frac{dm^D}{dt} = \frac{d(\rho^D \Omega_D)}{dt} = \dot{m}_2^D - \dot{m}_1^D N_P \quad (18)$$

$$\Omega_D(t=0) = \Omega_{D0}$$

where  $N_P$  represents the number of pellets in the system.

#### Heterogeneous system: relevance of the PSD of Cellets®

The PSD of Cellets®, shown in Figure 3, was implemented considering the radius of the Cellets® as a vector ( $\mathbf{R}_0$ ) whose components were the average dimensions of each class. The drug layer thickness ( $\mathbf{R}_{A0} \approx \mathbf{R}_{B0}$ ) was obtained considering a homogeneous drug distribution within all the particles classes, generating the same drug layer thickness (calculated in 6.3  $\mu\text{m}$ ). The external radii were calculated considering that all the sprayed Surelease® homogeneously covered the pellets.+

$$\mathbf{R}_0 = [242, 275, 313, 356, 404, 459] \mu\text{m} \quad (19)$$

$$\mathbf{R}_{A0} = \mathbf{R}_0 + 6.3 \mu\text{m} \quad (20)$$

$$\mathbf{R}_{C0} = \mathbf{R}_{A0} + [20 \text{ or } 30 \text{ or } 60] \mu\text{m} \quad (21)$$

Mathematical modeling of the drug release  
from an ensemble of coated pellets

D. CACCAVO, G. LAMBERTI, M.M. CAFARO, A.A. BARBA  
J. KAZLAUSKE, A. LARSSON

$$\frac{n_i}{n_{\text{tot}}} = [0.079, 0.335, 0.410, 0.155, 0.020, 0.001] \quad (22)$$

The ratio  $n_i/n_{\text{tot}}$  represents the numerical fraction distribution of the Cellets® (Figure 3) that become, with the assumptions made, also the numerical fraction distribution of the pellets.

In this case the ODEs given by eq. (1), (3), (4), (5), (8), (9), (10) have to be solved for each of the six classes, whereas the mass balance in the dissolution medium ( $\Omega_D$ ), eq. (13), (14) and (15), become:

$$\frac{dm_2^D}{dt} = \frac{d(\rho^D \omega_2^D \Omega_D)}{dt} = \sum_i N_i 4\pi R_{C,i}^2 K_{2,i}^{CD} (\rho_i^C \omega_{2,i}^C - \rho^D \omega_2^D) = m_2^D \quad (23)$$

$$\omega_2^D(t=0) = \omega_{20}^D$$

$$\frac{dm^D}{dt} = \frac{d(\rho^D \Omega_D)}{dt} = m_2^D - m_1^D \quad (24)$$

$$\Omega_D(t=0) = \Omega_{D0}$$

$$m_1^D = \sum_i N_i 4\pi R_{C,i}^2 K_{1,i}^{CD} (m_1^{CD} \rho^D \omega_1^D - \rho_i^C \omega_{1,i}^C) \quad (25)$$

where  $N_i$  is the number of pellets in the  $i$ -th class. Therefore the system to solve is made of  $6 \times 7 + 2 = 44$  ODEs.

#### *Heterogeneous system: relevance of the SD of the coating thickness*

Unlike the drug layer thickness, where the average thickness dimension can be estimated from the effective drug loading and the SD at that small values does not play a crucial rule, the SD of the polymeric coating thickness can have a great influence on drug release. This layer indeed is the limiting step, and it tunes the drug transport preventing a burst release. Its thickness, along with its resistance to the species transport, is strongly related to the drug mass flux. Thicker coatings reduce the mass fraction gradient and then the drug mass flux. On the other hand, thinner coatings increase the mass fraction gradient and thus the drug mass flux. From Figure 4 it is evident that there is a thickness distribution along a single pellet as well as between pellets.

In this work it has been supposed that this intra- and inter-particles film thickness ( $f_t$ ) distribution can be described using a Gaussian distribution, eq. (26), in which  $\mu$  and  $\sigma$  represent the mean and the standard deviation of the distribution (the approach is not constrained to this type of distribution, other distribution functions could be implemented to describe the real case). The cumulative distribution function is known, eq. (27), and dividing the interval  $[0 - 3\mu]$  in 10 classes with the same amplitude, it is possible to obtain the numerical fraction of particles in the  $i$ -th class, eq. (28), of interval  $[f_t^*(i+1), f_t^*(i)]$  characterized by the film thickness  $f_t^{\text{mean}(i)}$ , eq. (29). At this point, similarly to the previous case, the radii can be expressed by vectors (of 10 components) where the  $i$ -th class will be different only for the film thickness, eq. (30-32).

$$q_0(f_t | \mu, \sigma) = \frac{1}{\sigma\sqrt{2\pi}} e^{-\frac{(f_t - \mu)^2}{2\sigma^2}} \quad (26)$$

$$Q_0(f_t^* | \mu, \sigma) = \int_{-\infty}^{f_t^*} q_0(f_t | \mu, \sigma) df_t = \frac{1}{2} \left[ 1 + \text{erf} \left( \frac{f_t^* - \mu}{\sigma\sqrt{2}} \right) \right] \quad (27)$$

$$\frac{n_i}{n_{\text{tot}}} \Big|_{f_t^{\text{mean}(i)}} = [Q_0(f_t^*(i+1) | \mu, \sigma) - Q_0(f_t^*(i) | \mu, \sigma)]_{i=1 \dots N-1} \quad (28)$$

$$f_t^{\text{mean}}(i) = \left( \frac{f_t^*(i+1) + f_t^*(i)}{2} \right) \Big|_{i=1 \dots N-1} \quad (29)$$

$$(R_0)_{i=1 \dots 10} = 300 \mu\text{m} \quad (30)$$

$$R_{A0} = R_0 + 6.3 \mu\text{m} \quad (31)$$

$$R_{C0} = R_{A0} + f_t^{\text{mean}} \mu\text{m} \quad (32)$$

The so formulated model is a system of 72 ODEs.

### 2.7.4 Model numerical solution

The model consists of a system of ordinary differential equations (ODEs) that was numerically solved in MATLAB R2014B, with the ode15s solver (Shampine & Reichelt, 1997). The initial conditions for the single pellet model are reported in Table 2, whereas the modification of these conditions for the ensemble of pellets model can be found within the text (section 2.7.3). The MATLAB code is available as supplementary material.

## 3. Results

### 3.1 Experimental results

#### 3.1.1 Drug release from ensembles of pellets

The experimental results showing the drug release of the ensembles of pellets are reported in Figure 2 and discussed in detail in (Kazlauske et al., submitted).

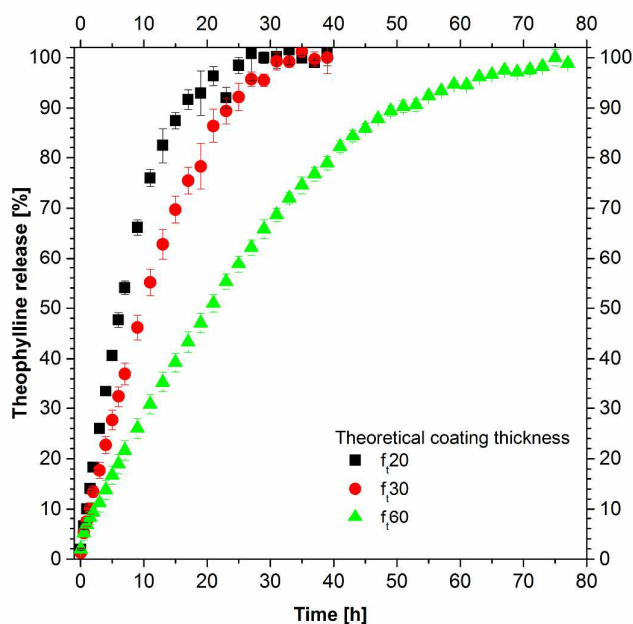


Figure 2. Experimental drug release from ensembles of pellets (500 mg) for three different theoretical coating thicknesses (Kazlauske et al., submitted).

The release curves (Figure 2) show a constant release rate (zero order release) up to 80% of released drug, followed by a substantial release rate decrease. The increase of the polymeric film thickness decreases the drug release rate.

### 3.1.2 Surelease film properties

#### *Diffusivity of water and Theophylline in the Surelease film*

The water and the Theophylline diffusion coefficients in the Surelease film were of  $1.99 \times 10^{-12} \pm 0.14 \times 10^{-12}$  [m<sup>2</sup>/s] and  $3.1 \times 10^{-13} \pm 0.32 \times 10^{-13}$  [m<sup>2</sup>/s], respectively. These values were used in the model to describe the diffusion of water and drug in the Surelease coating layer ( $\Omega_C$ ), indicated with  $D_1^C$  and  $D_2^C$  in Table 1.

#### *Swelling of the Surelease film*

The recorded increase of weight in the Surelease free film immersed distilled water was around 20% w/w at equilibrium conditions.

### 3.1.3 PSD of Cellets®

The cumulative mass distribution is reported in Figure 3, calculated starting from the mass distribution. The results, in accordance with the Cellets® producer, show a quite narrow PSD, with the major amount of particles with diameters between 500-750  $\mu\text{m}$ . The numerical fraction will be used in order to evaluate the effect of the PSD of Cellets® on the drug release behavior.

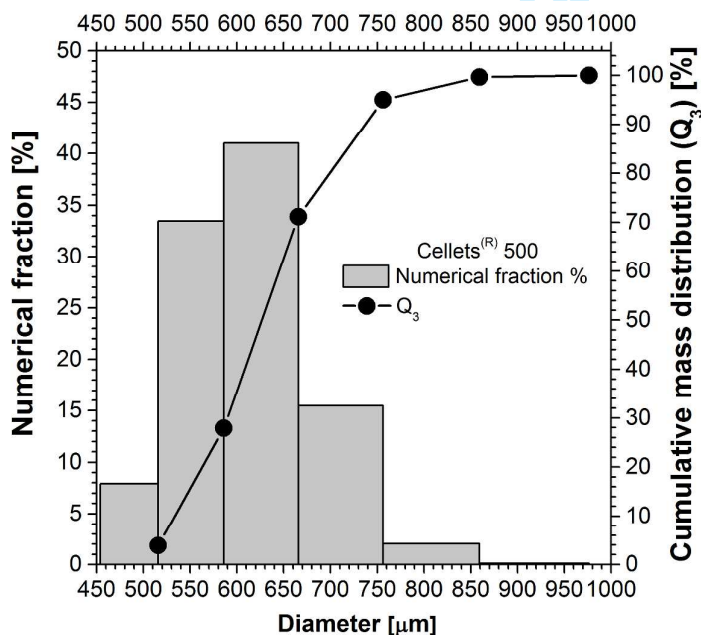


Figure 3. Particle size distribution (PSD) of Cellets® 500 in terms of cumulative mass distribution and numerical fraction.

### 3.1.4 Polymer and drug layer thickness

Both the methods of preparation and analysis, described in section 2.6, to evaluate the thickness of the polymeric layer were able to display an intra- and inter- particle (i.e. between different particles and within the layer covering the same particle) inhomogeneity. This implies the presence of a thickness distribution along a single pellet as well as between pellets.

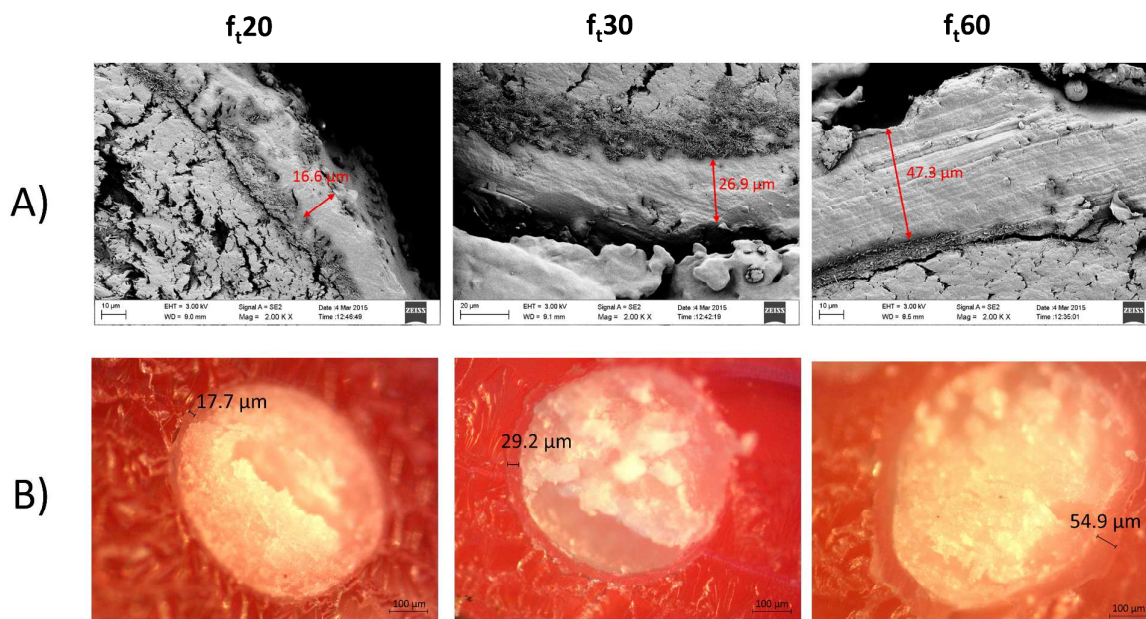


Figure 4. Polymeric layer thickness inhomogeneity. A) SEM images of pellets cross sections. B) Optical microscope images of pellets cross sections. On the left, center and right the pellets with theoretical film thickness of 20, 30, and 60  $\mu\text{m}$  respectively.

The drug layer thickness was estimated considering the effective drug mass loaded on the pellets, which was calculated from the release tests. Considering that the ratio of Theophylline:HPMC (90:10 w/w) was maintained, the thickness was calculated for Cellets<sup>®</sup> of same dimensions (single pellet case, section 2.7.2) or for PSDs of Cellets<sup>®</sup> (section 2.7.3). In the last case, in which the PSDs of Cellets<sup>®</sup> was considered, the assumption of uniform drug layer thickness within the PSD classes was made.

### 3.2 Single pellet model results

The system of 9 ODEs with the initial conditions (ICs) reported in Table 2 were simultaneously solved. The IC for the drug layer radius ( $R_{A0}$ ) was calculated from the effective drug amount loaded on the pellets, obtained from the drug release tests. IC for the coating layers  $R_{C0}$  was calculated **considering a uniform covering efficiency of 100%**. In the following the radii and the drug mass fraction evolution, which are of main interest, within the system will be shown. However, with this modeling approach, the time evolution of all the other mass fractions as well as the single species mass evolution can be obtained.

The single pellet radii evolutions for a polymer coating thickness of 20  $\mu\text{m}$  ( $f_{t20}$ ) are shown in Figure 5. The radius of the solid layer  $R_A$  linearly decreases with time until the complete dissolution, at the critical time  $t_c$ . The liquid layer radius  $R_B$  increases mainly due to the water inlet. The external pellet radius  $R_C$  promptly absorbs water and swells; after that it increases due to the increase of the internal liquid layer. This leads to the stretching of the polymeric coating, with the reduction of its thickness ( $R_C - R_B$  decreases).

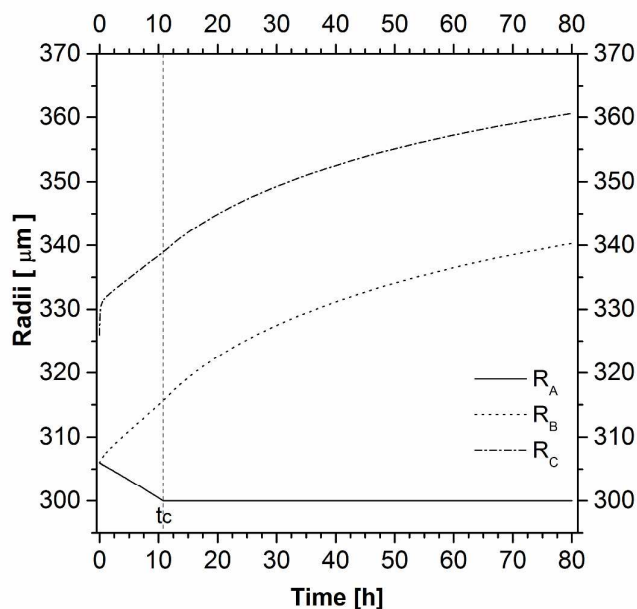


Figure 5. Radii evolution during the dissolution process for initial polymer coating thickness of 20  $\mu\text{m}$ .

In Figure 6 the drug mass fraction evolutions in the domains  $\Omega_B$ ,  $\Omega_C$ , and  $\Omega_D$  during the dissolution process are reported.

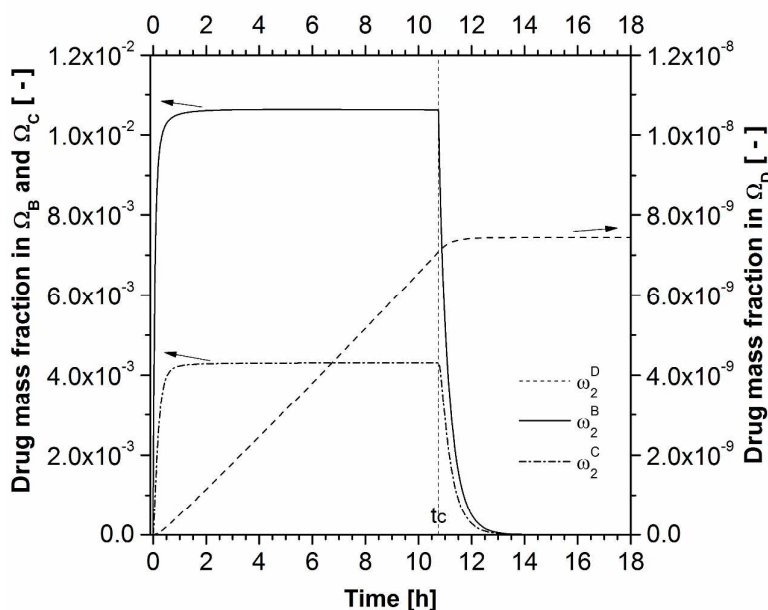


Figure 6. Drug mass fraction evolution in the several domains during the dissolution process for initial polymer coating thickness of 20  $\mu\text{m}$ .

Within the first hour, the drug mass fraction in the liquid layer ( $\omega_2^B$ ) reaches the saturation conditions and stays at that value, thanks to the solid layer dissolution, until the critical time  $t_c$ . At that point, the solid drug reservoir is finished and the mass fraction starts to decrease. The drug mass fraction in the polymeric coating ( $\omega_2^C$ ) follows the same trend of  $\omega_2^B$ , reaching a constant value that is a function of the ease of drug

transport within the system. The drug mass fraction in  $\Omega_D$  increases until reaching a constant value that represents the total initial amount of drug in one pellet in 1 L of dissolution medium.

### 3.3 Ensemble of pellets model results

#### Homogeneous system

This model, constituted by eq. 1-12 and 16-18, was first tuned to reproduce the experimental results of the pellets with theoretical polymer thickness of 20  $\mu\text{m}$  ( $f_{t,20}$ ). The drug diffusion in  $\Omega_C$  was used as the only fitting parameter and it was increased by a factor 2 to optimize the description of the experimental results. The so tuned model was applied to the systems with pellets of different coating thickness (Figure 7).

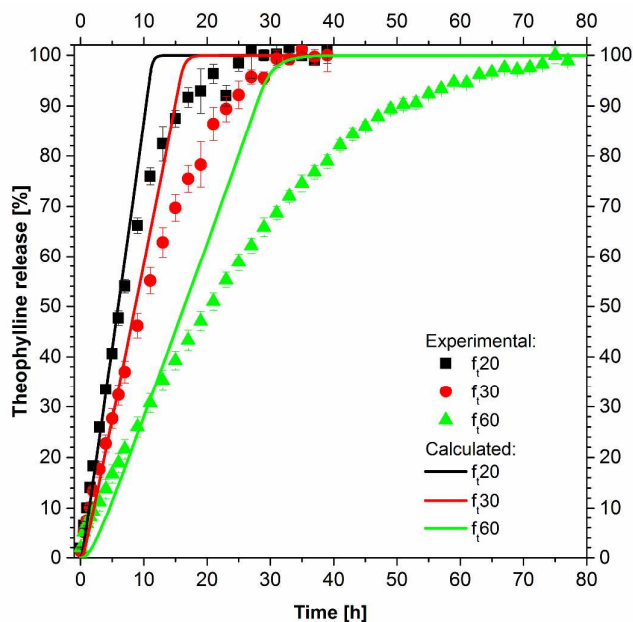


Figure 7. Drug release from ensembles of homogeneous pellets.

The calculated drug release shows a zero order behavior for all the types of pellets and during all the dissolution process. Despite the prediction being fair in the first hours, the model is not able to properly describe the experimental results when the drug release rate decreases.

#### Heterogeneous system

##### Relevance of the PSD of Cellets®

The model utilized in this section is constituted by eq. 1-12, 16, and 19-25. Each class of pellets presents its fractional drug release that contributes to the average release (that is the characteristic release of the dose or, in other terms, the release that would be experimentally recorded). In Figure 8 the results in terms of release from the single class (individuated by eq. (19)) as well as in terms of average release from the different polymeric layers are shown. The model parameters were kept the same as in the homogeneous system model.

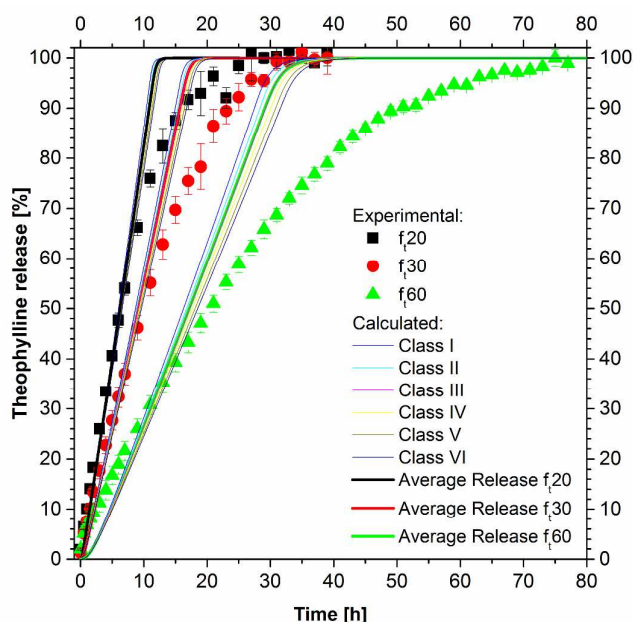


Figure 8. Drug release from ensembles of pellets where the inert core presents a PSD described with 6 classes defined by eq. (20).

The drug release from the different classes is minimal, generating an average drug release similar to the case of homogeneous system.

#### Relevance of the SD of the coating thickness

The model, based on eq. 1-12, 16, and 23-32, was tuned on the experimental drug release of the pellets with theoretical film thickness of 30  $\mu\text{m}$  ( $f_t30$ ) ( $R^2=0.995$ ). The transport parameters were used as found in literature or experimentally (Table 1) using as fitting parameters the mean and the standard deviation of the film thickness distribution,  $\mu$  and  $\sigma$ . The best fitting parameters were  $\mu_{\text{fitting}} = 20 \mu\text{m}$  and  $\sigma_{\text{fitting}} = 7.5 \mu\text{m}$ . In Table 3 the size distribution of the film thickness is reported: the most populated classes, in terms of numerical fraction  $n_i/n_{\text{tot}}|f_t^{\text{mean}(i)}$  [%], are between the second and the sixth classes. The drug release from the  $i$ -th class, as well as the average release, are shown in Figure 9.

Table 3. Film thickness distribution.

Class	$f_t20$	$f_t30$	$f_t60$	$n_i/n_{\text{tot}} f_t^{\text{mean}(i)}$ [%]
	$\mu_{\text{fitting}} = 13.3 \mu\text{m}$ $\sigma_{\text{fitting}} = 5 \mu\text{m}$	$\mu_{\text{fitting}} = 20 \mu\text{m}$ $\sigma_{\text{fitting}} = 7.5 \mu\text{m}$	$\mu_{\text{fitting}} = 40 \mu\text{m}$ $\sigma_{\text{fitting}} = 15 \mu\text{m}$	
	$f_t^{\text{mean}(i)}$ [ $\mu\text{m}$ ]	$f_t^{\text{mean}(i)}$ [ $\mu\text{m}$ ]	$f_t^{\text{mean}(i)}$ [ $\mu\text{m}$ ]	
I	1.95	3.00	6.00	2.71
II	5.85	9.00	18.00	11.20
III	9.75	15.00	30.00	25.18
IV	13.65	21.00	42.00	30.82
V	17.55	27.00	54.00	20.57
VI	21.45	33.00	66.00	7.48
VII	25.35	39.00	78.00	1.48
VIII	29.25	45.00	90.00	0.16
IX	33.15	51.00	102.00	0.01
X	37.05	57.00	114.00	0

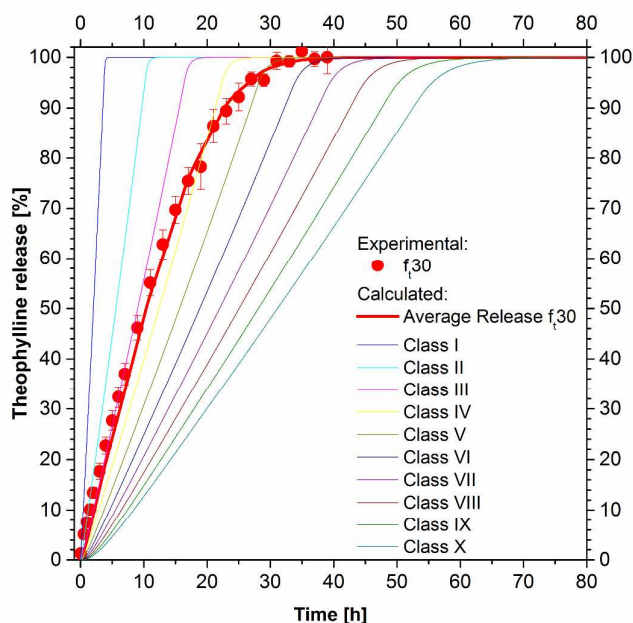


Figure 9. Drug release from an ensemble of pellets where the film thickness presents a size distribution.

This modeling approach does not require adjustable transport parameters, which were used as obtained from literature or experiments (Table 1), and requires two parameters for the description of the size distribution of the film thickness. These last two were successfully related to the initial theoretical film thickness, considering the results obtained for  $f_{t30}$ , as it follows:

$$\begin{aligned} \mu_{\text{fitting}} &= \frac{2}{3} f_t \\ \sigma_{\text{fitting}} &= \frac{3}{8} \mu_{\text{fitting}} = \frac{1}{4} f_t \end{aligned} \quad (33)$$

In this way a fully predictive model was obtained and tested on the other two systems:  $f_{t20}$  and  $f_{t60}$ , whose film thickness distribution is reported in Table 3. The modeling results, in terms of average release, are reported in Figure 10 and compared to the experimental data.

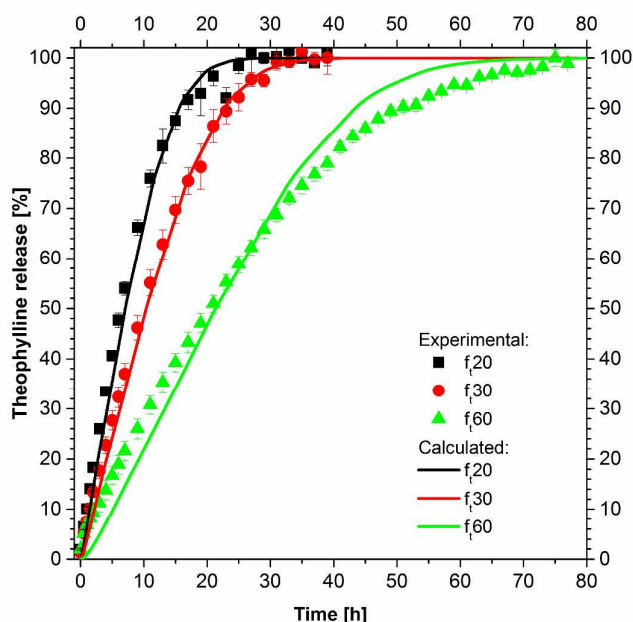


Figure 10. Drug release from ensembles of pellets with a SD of the film thickness and predictive modeling results for  $f_{t20}$  and  $f_{t60}$ .

The agreement is very good for  $f_{t20}$  ( $R^2=0.991$ ) and satisfactorily good for  $f_{t60}$  ( $R^2=0.981$ ), confirming that the consideration of a film thickness distribution is crucial in understanding and modeling the drug release from pellets.

#### 4. Discussion and Conclusions

In this work a mathematical model for the description of the drug release from an ensemble of coated pellets was proposed, implemented and successfully compared to experimental results. A layered lumped parameters modeling approach was used to describe the single coated pellet behavior in terms of size and species' mass fraction time evolutions. The pellet was considered as built up by several time-dependent domains representing the inert core, the solid and liquid drug layers and the polymeric film coating. The time evolution of the dimensions of the pellet (Figure 5) shows that the water inlet, driven by the concentration difference between the external medium and the internal liquid layer, generates a volumetric deformation of the system. In particular water accumulates inside the pellet promoting further dissolution of solid drug. This water uptake leads to an overall increase of the pellet dimensions and to the stretching of the polymeric film layer, due to its limited swelling ability with respect to the inner part of the pellet. The analysis of the evolution of the drug mass fraction (Figure 6) within the pellet and in the external dissolution medium shows that the presence of water within the pellet consents to dissolve the solid drug up to its dissolution limit, value that is kept constant until the complete dissolution of the solid drug reserve. This clearly shows that, in this case, the drug dissolution is not a limiting step.

The single pellet model was successively extended to describe ensembles of pellets where different approaches to describe the system polydispersity were hypothesized and implemented. In particular, as the simplest approach, a perfectly homogeneous system of pellets was modeled, obtaining drug release kinetic of zero order, far from the experimental results (Figure 7). **To reproduce the experimental sigmoidal drug release results from ensembles of pellets drug diffusion coefficients function of the dissolution time could be used (i.e. Marucci et al. (2013)), based on the assumption that morphological changes of the polymeric**

film modify the diffusive process. In this work, supported by the morphological analyses pre- and post-dissolution (performed in Kazlauske et al. (submitted)) showing the absence of substantial modifications, this approach was rejected and the hypothesis of perfectly homogeneous system was found to be too simplistic to be able to reproduce the experimental results.

A more realistic modeling approach is to consider the heterogeneity of the ensemble of pellets. This can arise from several factors: the particle size distribution of the inert core, drug or polymer layer thickness distribution, and so forth. In particular in this work the impact of the PSD of Cellets® as well as the relevance of the polymeric coating thickness distribution was evaluated. The effect of the drug layer thickness distribution was disregarded a priori, considering the value calculated from the effective mass of drug loaded on the pellets a good estimation of the drug layer thickness. This assumption is justified considering that, in this work, this layer is of few micrometers and its distribution around this mean value would not affect substantially the results. In modeling the inert core SD (Figure 8) six classes were used, different in the inert core radius, reported in eq. (19). In modeling the film thickness SD (Figure 9 and Table 3) ten classes were used, which differ in the film thickness dimensions (reported in Table 3).

Analyzing the impact of the SD of Cellets® (Figure 8) it is evident that the difference in drug release from the different classes is minimal (the pellets classes differ for the Cellets® dimension only), and the average release does not differ from the drug release obtained considering the homogenous system. This can be explained considering that the mass flow rate of the *i*-th class ( $\dot{W}_{2i}$ ) is proportional to the inert core radius to the power of two, eq. (34). The drug release from the *i*-th class  $R_i(t)$ , considering eq. (36), can be expressed as the product of the drug mass flow rate times the dissolution time *t*, divided by the initial drug mass in the *i*-th class  $m_{20i}$ , eq. (38). This last is proportional to the inert core radius to the power of two, eq. (37), as the mass flow rate, therefore giving a drug release independent on the inert core radius, eq. (38).

$$\begin{aligned}\dot{W}_{2i} &\sim k\Delta\omega_2 4\pi R_{C,i}^2 = k\Delta\omega_2 4\pi (R_{0i} + \delta_A + \delta_B + \delta_C)^2 \approx k\Delta\omega_2 4\pi [R_{0i}^2 + 2R_{0i}(\delta_A + \delta_B + \delta_C)] = \\ &= k\Delta\omega_2 4\pi [R_{0i}^2 + 2R_{0i}(R_{C,i} - R_{0i})] = k\Delta\omega_2 4\pi R_{0i}^2 \left[ 2\frac{R_{C,i}}{R_{0i}} - 1 \right] \approx k\Delta\omega_2 4\pi R_{0i}^2\end{aligned}\quad (34)$$

$$m_{2i}(t) = m_{20i} - \dot{W}_{2i}t \quad (35)$$

$$R_i(t) = \frac{m_{20i} - m_{2i}}{m_{20i}} = \frac{\dot{W}_{2i}}{m_{20i}}t \quad (36)$$

$$m_{20i} = \omega_{20}\rho_A \frac{4}{3}\pi (R_{A0i}^3 - R_{0i}^3) = \omega_{20}\rho_A \frac{4}{3}\pi [(R_{0i} + \delta_{A0})^3 - R_{0i}^3] \approx \omega_{20}\rho_A \frac{4}{3}\pi R_{0i}^2 \delta_{A0} \quad (37)$$

$$R_i(t) \approx \frac{k\Delta\omega_2 4\pi}{\omega_{20}\rho_A \frac{4}{3}\pi \delta_{A0}}t \quad (38)$$

From this analysis it is evident that the PSD of Cellets®, under the hypotheses of homogeneous drug and polymer layers thickness within the classes, has a negligible impact on the produced pellets. However, inert cores with narrow PSD should always be preferred since they can be easier fluidized and can ensure a more homogeneous layering.

Mathematical modeling of the drug release  
from an ensemble of coated pellets

D. CACCAVO, G. LAMBERTI, M.M. CAFARO, A.A. BARBA  
J. KAZLAUSKE, A. LARSSON

Analyzing the impact of the SD of the polymeric film thickness on the drug release (Figure 9) it can be seen that the classes of pellets representing lower film thicknesses promptly release the Theophylline while the release rate decreases due to increasing the film thickness (at higher value of the class number). The resulting average release, which accounts for the contribution of all the classes, is able to reproduce the experimental results that deviate from a zero order release behavior. Similarly, Donbrow, Hoffman and Benita (1988) using a simple statistical model (in which the distribution of up to three parameters was assumed and arbitrary varied: payload, payload release time and release rate constant), theoretically demonstrated that the ensemble release rate, different from a kinetic of zero order, could be obtained from single pellets release of zero order, considering the parameters distribution of the ensemble. In this work, by using a mechanistic model and analyzing the distribution of physical quantities (inert core dimension, film thickness distribution), it has been demonstrated that some features (i.e the film thickness distribution) could have more impact than others (i.e. inert core radius) on the drug release behavior.

The drug release from an ensemble of pellets with a theoretical film thickness of  $30\ \mu\text{m}$  ( $f_t30$ ) was firstly described (Figure 9) using as only fitting parameter the film thickness dimension (average thickness and its standard deviation, assuming a Gaussian distribution). The values of the fitting parameters resulting from the optimization procedure were successfully related to the theoretical film thickness, eq. (33), demonstrating that the average thickness able to describe the drug release was lower than the theoretical thickness, as for the drug coating, confirming that the experimental efficiency of layering was lower than unity. Moreover the correlation to the theoretical thickness allowed to obtain a predictive model capable of describing the drug release from other ensembles of pellets with different theoretical film thickness (Figure 10), demonstrating that the right physical phenomena were considered and described.

In conclusion in this work a mechanistic model for the description of drug release from a single coated pellet as well as from polydisperse ensemble of pellets was developed, implemented and successfully compared to experimental results. Both the models, the single pellet model and the ensemble of pellets model, could be successfully used to describe and predict the drug release from these systems. Moreover the results of the ensemble of pellets model clearly demonstrated that the SD of the inert core has minimal impact on the drug release whereas the polymeric film thickness distribution plays the major role, pointing it out as a key parameter to control in the production of pellets-based systems.

Mathematical modeling of the drug release  
from an ensemble of coated pellets

D. CACCAVO, G. LAMBERTI, M.M. CAFARO, A.A. BARBA  
J. KAZLAUSKE, A. LARSSON

---

## 5. References

Abrahamsson B, Alpsten M, Jonsson UE, Lundberg PJ, Sandberg A, Sundgren M, *et al.* (1996). Gastro-intestinal transit of a multiple-unit formulation (metoprolol CR/ZOK) and a non-disintegrating tablet with the emphasis on colon. *Int J Pharm* 140: 229-235.

Bird RB, Stewart WE, & Lightfoot EN (2007) *Transport Phenomena*. Wiley: USA.

Borgquist P, Nevsten P, Nilsson B, Wallenberg LR, & Axelsson A (2004). Simulation of the release from a multiparticulate system validated by single pellet and dose release experiments. *J Control Release* 97: 453-465.

Borgquist P, Zackrisson G, Nilsson B, & Axelsson A (2002). Simulation and parametric study of a film-coated controlled-release pharmaceutical. *J Control Release* 80: 229-245.

Caccavo D, Cascone S, Lamberti G, & Barba AA (2015). Controlled drug release from hydrogel-based matrices: Experiments and modeling. *Int J Pharm* 486: 144-152.

Dappert T, & Thies C (1978). Statistical models for controlled release microcapsules: rationale and theory. *J Membrane Sci* 4: 99-113.

Donbrow M, Hoffman A, & Benita S (1988). Variation of population release kinetics in polydisperse multiparticulate systems (microcapsules, microspheres, droplets, cells) with heterogeneity of one, two or three parameters in the population of individuals. *J Pharm Pharmacol* 40: 93-96.

Grassi M, Colombo I, & Lapasin R (2000). Drug release from an ensemble of swellable crosslinked polymer particles. *J Control Release* 68: 97-113.

Grassi M, Colombo I, & Lapasin R (2001). Experimental determination of the theophylline diffusion coefficient in swollen sodium-alginate membranes. *J Control Release* 76: 93-105.

Grassi M, Grassi G, Lapasin R, & Colombo I (2006) *Understanding drug release and absorption mechanisms: a physical and mathematical approach*. CRC Press: Boca Raton, FL, USA.

Gross ST, Hoffman A, Donbrow M, & Benita S (1986). Fundamentals of Release Mechanism Interpretation in Multiparticulate Systems - the Prediction of the Commonly Observed Release Equations from Statistical Population-Models for Particle Ensembles. *Int J Pharm* 29: 213-222.

Holz M, Heil SR, & Sacco A (2000). Temperature-dependent self-diffusion coefficients of water and six selected molecular liquids for calibration in accurate 1H NMR PFG measurements. *Phys Chem Chem Phys* 2: 4740-4742.

Kaunisto E, Marucci M, Borgquist P, & Axelsson A (2011). Mechanistic modelling of drug release from polymer-coated and swelling and dissolving polymer matrix systems. *Int J Pharm* 418: 54-77.

Mathematical modeling of the drug release  
from an ensemble of coated pellets

D. CACCAVO, G. LAMBERTI, M.M. CAFARO, A.A. BARBA  
J. KAZLAUSKE, A. LARSSON

---

Kazlauske J, Cafaro MM, Caccavo D, Marucci M, Lamberti G, Barba AA, *et al.* (submitted). Determination of the release mechanism for Theophylline from pellets coated with Surelease - a water dispersion of ethylcellulose. *Int J Pharm.*

Manca D, & Rovaglio M (2003). Modeling the controlled release of microencapsulated drugs: theory and experimental validation. *Chem Eng Sci* 58: 1337-1351.

Marucci M, Andersson H, Hjartstam J, Stevenson G, Baderstedt J, Stading M, *et al.* (2013). New insights on how to adjust the release profile from coated pellets by varying the molecular weight of ethyl cellulose in the coating film. *Int J Pharm* 458: 218-223.

Noyes AA, & Whitney WR (1897). The Rate of Solution of Solid Substances in Their Own Solutions. *J Am Chem Soc* 19: 930-934.

Serajuddin ATM, & Jarowski CI (1985). Effect of Diffusion Layer pH and Solubility on the Dissolution Rate of Pharmaceutical Acids and Their Sodium Salts II: Salicylic Acid, Theophylline, and Benzoic Acid. *J Pharm Sci* 74: 148-154.

Shampine LF, & Reichelt MW (1997). The MATLAB ODE suite. *Siam J Sci Comput* 18: 1-22.

Siepmann F, Siepmann J, Walther M, MacRae RJ, & Bodmeier R (2008). Polymer blends for controlled release coatings. *J Control Release* 125: 1-15.

## 6. Author contributions

Diego CACCAVO: contributed to establish the model, wrote the code, run the simulations; Maria Margherita CAFARO: performed the experiments, analyzed the data; Anna Angela BARBA: supervised the modeling work, organized the data; Jurgita KAZLAUSKE: organized the experimental work; Anette LARSSON: had the basic idea, organized the experiments, supervised the experimental work; Gaetano LAMBERTI: contributed to establish the model, organized optimization strategies. All the authors contributed in the writing and in the editing of the manuscript.

## 7. Competing Interests' Statement

The Authors declare that there is no competing interests.

```

%Everything is in SI units"
function Single_pellet_model
clear all

%Initial geometry
R0=300E-6; Rb0=300E-6+6E-6; Ra0=Rb0-2E-9; Rc0=Rb0+30E-6;

%Dissolution Time [s]
TIME=80*3600;
%Densities [kg/m^3]
rho10=1000; rho20=1200; rho30=1200; rho40=1200;

%Diffusivities [m^2/s]
D2b=1.5E-10; % from doi:10.1016/j.ijpharm.2015.03.054
D1b=2.2E-9; % from doi:10.1016/j.ijpharm.2015.03.054
D2c=2*3.2E-13; % from Kazlauske et al. (submitted)
D1c=1.99E-12; % from Kazlauske et al. (submitted)
D2d=8.21E-10; % from doi:10.1016/S0168-3659(01)00424-2
D1self=3E-9; % from doi:10.1039/B005319H
%See the Transport coefficients definition

%Initial mass fractions
%Domain A
w2sat=0.0115; % from doi:10.1002/jps.2600740209
w2a0=0.9; w3a0=1-w2a0;
%Domain B
w2b0=0;
w3b0=0;
%Domain C
w4c0=1;
w2c0=0;
rhoc0=(1-w2c0-w4c0)/rho10+w2c0/rho20+w4c0/rho40)^(-1);
%Domain D
w2d0=0; w1d0=1-w2d0;

Omegad0=1E-3; % Initial dissolution medium [m^3]
Np=5000; % Total number of pellets

function dy = odesystem (t,y)
dy=zeros(9,1); %Initialization

Ra=y(1);
w2b=y(2);
Rb=y(3);
w2c=y(4);
Rc=y(5);
w2d=y(6);
Omegad=y(7);
w3b=y(8);
w4c=y(9);
rhoa=(w2a0/rho20+w3a0/rho30)^(-1); %Density of domain A OK
rhob=((1-w2b-w3b)/rho10+w2b/rho20+w3b/rho30)^(-1); %Density of domain B OK
rhoc=((1-w2c-w4c)/rho10+w2c/rho20+w4c/rho40)^(-1); %Density of domain C OK
rhod=((1-w2d)/rho10+w2d/rho20)^(-1); %Density of domain D OK
w1b=1-w2b-w3b; %OK
w1c=1-w2c-w4c; %OK
w1d=1-w2d; %OK

%////Stop condition when Ra reach R0 or when there is not enough water

```

```

w2bStar=w2b/(w1b+w2b);
kdiss0=D2b/Ra;
if Ra>R0 && (w2sat-w2bStar)>0
    kdiss=kdiss0;
else
    kdiss=0;
end
%%%%%%%%%%%%%%%%%%%%%%%%%%%%%%%%%%%%%%%%%%%%%%%%%%%%%%%%%%%%%%%%%%%%%%%%

%%%%%%%%%%%%%%%%%%%%%%%%%%%%%%%%%%%%%%%%%%%%%%%%%%%%%%%%%%%%%%%%%%%%%%%%
%///////Transport coefficients////////////////////////////////
k2b=D2b/(Rb-Ra);
k2c=D2c/(Rc-Rb);
k2d=D2d/Rc;
U2b=(1/(k2b)+1/(k2c))^( -1);
U2c=(1/(k2c)+1/(k2d))^( -1);
k1b=D1b/(Rb-Ra);
k1c=D1c/(Rc-Rb);
m1=4.95; %w1b=m1*w1c
U1b=(1/(k1b)+m1/(k1c))^( -1);
k1d=D1self/Rc;
m2=0.2; %w1c=m2*w1d
K1c=(1/(k1c)+m2/(k1d))^( -1);

%%%%%%%%%%%%%%%%%%%%%%%%%%%%%%%%%%%%%%%%%%%%%%%%%%%%%%%%%%%%%%%%%%%%%%%%

%///////Parameters defined during the ODEs
rearrangement////////////////////////////////////
rho2b3=rho10*rho20-rho20*rho30; %OK
rho2b2=rho10*rho30-rho20*rho30; %OK
rhostar=(rho20*rho30*(1-w2b-w3b)+rho10*rho30*w2b+rho10*rho20*w3b)^2/(rho10*rh
o20*rho30); %OK
alfa=w3b*(rho2b2/rhostar)/(rhob-w3b*rho2b3/rhostar); %OK
beta=-rhob*w3b^3*Rb^2/((Rb^3-Ra^3)*(rhob-w3b*rho2b3/rhostar)); %OK
gamma=rhob*w3b^3*Ra^2/((Rb^3-Ra^3)*(rhob-w3b*rho2b3/rhostar)); %OK
delta=3*Ra^2*rhob*kdiss*w3a0*(w2sat-w2bStar)/(w2a0*(Rb^3-Ra^3)*(rhob-w3b*rho2
b3/rhostar)); %OK
lambda=3*Rb^2*rhob-(Rb^3-Ra^3)*beta*rho2b3/rhostar; %OK
chsi=3*Ra^2*rhob+gamma*(Rb^3-Ra^3)*rho2b3/rhostar; %OK
eps=rho2b2/rhostar*(Rb^3-Ra^3)+rho2b3*alfa*(Rb^3-Ra^3)/rhostar; %OK
zeta=(Rb^3-Ra^3)*rho2b3*delta/rhostar+3*Rb^2*U1b*(m1*w1c*rhoc-w1b*rhob)-3*Rb^
2*U2b*(w2b*rhob-w2c*rhoc)+3*Ra^2*kdiss*rhob*(w2sat-w2bStar)/w2a0; %OK
fi=rhob*(Rb^3-Ra^3)-w2b*(Rb^3-Ra^3)*(rho2b2/rhostar+rho2b3*alfa/rhostar)+eps/
lambda*(rhob*w2b^3*Rb^2-w2b*(Rb^3-Ra^3)*beta*rho2b3/rhostar); %OK
eta=-(-rhob*w2b^3*Ra^2-w2b*(Rb^3-Ra^3)*rho2b3*gamma/rhostar+chsi/lambda*(rhob
*w2b^3*Rb^2-w2b*(Rb^3-Ra^3)*rho2b3*beta/rhostar)); %OK
tau=-zeta/lambda*(rhob*w2b^3*Rb^2-w2b*(Rb^3-Ra^3)*rho2b3*beta/rhostar)+w2b*(R
b^3-Ra^3)*rho2b3*delta/rhostar+3*Ra^2*kdiss*rhob*(w2sat-w2bStar)-3*Rb^2*U2b*(
w2b*rhob-w2c*rhoc); %OK
a=rho40*(rho10-rho20); %OK
b=rho20*(rho10-rho40); %OK
rhocstar=(rho20*rho40*(1-w2c-w4c)+rho10*rho40*w2c+rho10*rho20*w4c)^2/(rho10*r
ho20*rho40); %OK
A1=rhoc*(Rc^3-Rb^3)-b*w4c*(Rc^3-Rb^3)/rhocstar; %OK
B1=-rhoc*w4c^3*Rc^2; %OK
C1=3*Rb^2*rhoc*w4c/lambda*(chsi+eps*eta/fi); %OK
D1=a*w4c*(Rc^3-Rb^3)/rhocstar; %OK
E1=3*Rb^2*rhoc*w4c/lambda*(eps*tau/fi+zeta); %OK
F1=3*rhoc*Rc^2-(Rc^3-Rb^3)*b*B1/(rhocstar*A1); %OK
G1=rhoc*3*Rb^2*(chsi/lambda+eps*eta/(lambda*fi))+(Rc^3-Rb^3)*b*C1/(rhocstar*A

```



```

w2d=y(:,6);
w1d=1-y(:,6);
Omegad=y(:,7);

dsfilm=Rc-Rb;
swelling=(Rc-Rc0)/Rc0*100;

rhod=((1-w2d)/rho10+w2d/rho20).^(-1);
rhob=((1-w2b-w3b)/rho10+w2b/rho20+w3b/rho30).^(-1);

Omegaa0=4/3*pi*(Ra0^3-R0^3);
m20a=w2a0*rho20*Omegaa0*Np;
m20=m20a;

m2d=w2d.*rhod.*Omegad;
m2d0=w2d0*((1-w2d0)/rho10+w2d0/rho20)^(-1)*Omegad0;

Omegab=4/3*pi.*(Rb.^3-Ra.^3);
m2b=(w2b.*rhob.*Omegab).*Np;

Omegaa=4/3*pi.*(Ra.^3-R0^3);
m2a=(w2a0*rho20.*Omegaa).*Np;

release=(m2d-m2d0)/m20;

%//////////Figures//////////

figure
plot(t/3600,Ra*10^6,'-',t/3600,Rb*10^6,'--',t/3600,Rc*10^6,'.')
title('Radii evolution')
xlabel('Time [h]')
ylabel('Radius [um]')
legend('Ra','Rb','Rc')

figure
%plot(t/3600,w1b,'-',t/3600,w2b,'-',t/3600,w3b,'-')
plot(t/3600,w2b,'-')
title('Mass fractions in OmegaB')
xlabel('Time [h]')
ylabel('Mass fraction [-]')
legend('w2b')

figure
%plot(t/3600,w1c,'-',t/3600,w2c,'-',t/3600,w4c,'-')
plot(t/3600,w2c,'-')
title('Mass fractions in OmegaC')
xlabel('Time [h]')
ylabel('Mass fraction [-]')
legend('w2c')

figure
%plot(t/3600,w1d,'-',t/3600,w2d,'-')
plot(t/3600,w2d,'-')
title('Mass fractions in OmegaD')
xlabel('Time [h]')
ylabel('Mass fraction [-]')
legend('w2d')

figure

```

```
plot(t/3600,m2a*10^6,'-r',t/3600,m2b*10^6,'-g',t/3600,m2d*10^6,'-b')
title('Drug Mass in the system')
xlabel('Time [h]') % x-axis label
ylabel('Mass [mg]') % y-axis label
legend('m2a','m2b','m2d')
```

```
%//////////End Figures//////////
```

```
end
```

For Peer Review

```

%Everything is in SI units"
function Whole_dose_Cellets_PSD
clear all

%Initial geometry

R0=[242E-6, 275E-6, 313E-6, 356E-6, 404E-6, 459E-6];
Rb0=R0+6.3E-6;
Ra0=Rb0-1E-8;
filmt=30E-6;
Rc0=Rb0+filmt;

%Dissolution Time [s]
TIME=80*3600;
%Densities [kg/m^3]
rho10=1000; rho20=1200; rho30=1200; rho40=1200;

%Diffusivities [m^2/s]
D2b=1.5E-10; % from doi:10.1016/j.ijpharm.2015.03.054
D1b=2.2E-9; % from doi:10.1016/j.ijpharm.2015.03.054
D2c=2*3.2E-13; % from Kazlauske et al. (submitted)
D1c=1.99E-12; % from Kazlauske et al. (submitted)
D2d=8.21E-10; % from doi:10.1016/S0168-3659(01)00424-2
D1self=3E-9; % from doi:10.1039/B005319H
%See the Transport coefficients definition

%Initial mass fractions
%Domain A
w2sat=0.0115; % from doi:10.1002/jps.2600740209
w2a0=0.9; w3a0=1-w2a0;
%Domain B
w2b0=0;
w3b0=0;
%Domain C
w4c0=1;
w2c0=0;
rhoc0=((1-w2c0-w4c0)/rho10+w2c0/rho20+w4c0/rho40)^(-1);
%Domain D
w2d0=0; %w1d0=1-w2d0;

Omegad0=1E-3; % Initial dissolution medium [m^3]
Ntot=5000; % Total Number of pellets
Np=[0.079, 0.334, 0.410, 0.154, 0.020, 0.001]*Ntot; %Number of pellets in each
class

function dy = odesystem (t,y)
dy=zeros(44,1); %Initialization
Ra= [y(1),y(8), y(15),y(22),y(29),y(36)];
w2b=[y(2),y(9), y(16),y(23),y(30),y(37)];
Rb= [y(3),y(10),y(17),y(24),y(31),y(38)];
w2c=[y(4),y(11),y(18),y(25),y(32),y(39)];
Rc= [y(5),y(12),y(19),y(26),y(33),y(40)];
w3b=[y(6),y(13),y(20),y(27),y(34),y(41)];
w4c=[y(7),y(14),y(21),y(28),y(35),y(42)];
w2d=y(43);
Omegad=y(44);

rhoa=(w2a0/rho20+w3a0/rho30)^(-1); %Density of domain A OK
rhob=((1-w2b-w3b)/rho10+w2b/rho20+w3b/rho30).^(-1); %Density of domain B OK
rhoc=((1-w2c-w4c)/rho10+w2c/rho20+w4c/rho40).^(-1); %Density of domain C OK

```

```

rhod=((1-w2d)/rho10+w2d/rho20).^(-1); %Density of domain D OK
w1b=1-w2b-w3b; %OK
w1c=1-w2c-w4c; %OK
w1d=1-w2d; %OK

%////Stop condition when Ra reach R0 or when there is not enough water
w2bStar=w2b./(w1b+w2b);
kdiss0=D2b./Ra;
kdiss=[0,0,0,0,0,0]; %initialization kdiss

    if Ra(1)>R0(1) && (w2sat-w2bStar(1))>0
        kdiss(1)=kdiss0(1);
    else
        kdiss(1)=0;
    end

    if Ra(2)>R0(2) && (w2sat-w2bStar(2))>0
        kdiss(2)=kdiss0(2);
    else
        kdiss(2)=0;
    end

    if Ra(3)>R0(3) && (w2sat-w2bStar(3))>0
        kdiss(3)=kdiss0(3);
    else
        kdiss(3)=0;
    end

    if Ra(4)>R0(4) && (w2sat-w2bStar(4))>0
        kdiss(4)=kdiss0(4);
    else
        kdiss(4)=0;
    end

    if Ra(5)>R0(5) && (w2sat-w2bStar(5))>0
        kdiss(5)=kdiss0(5);
    else
        kdiss(5)=0;
    end

    if Ra(6)>R0(6) && (w2sat-w2bStar(6))>0
        kdiss(6)=kdiss0(6);
    else
        kdiss(6)=0;
    end
end
%////////////////////////////////////

%////////Transport coefficients////////
k2b=D2b./(Rb-Ra);
k2c=D2c./(Rc-Rb);
k2d=D2d./Rc;
U2b=(1./(k2b)+1./(k2c)).^(-1);
U2c=(1./(k2c)+1./(k2d)).^(-1);
k1b=D1b./(Rb-Ra);
k1c=D1c./(Rc-Rb);
m1=4.95; %w1b=m1*w1c
U1b=(1./(k1b)+m1./(k1c)).^(-1);
k1d=D1self./Rc;
m2=0.2; %w1c=m2*w1d
K1c=(1./(k1c)+m2./(k1d)).^(-1);

```



```

dw3b=alfa.*dw2b+beta.*dRb+gamma.*dRa+delta; %OK
dw2c=(M1.*dRa+N1)./L1; %OK
dRc=(G1.*dRa+H1.*dw2c+I1)./F1; %OK
dw4c=(B1.*dRc+C1.*dRa+D1.*dw2c+E1)./A1; %OK
dw2d= ...

Np(1)*4*pi*Rc(1)^2/(rhod*Omegad)*(w2d*K1c(1)*(m2*w1d*rhod-rhoc(1)*w1c(1))+(1-w2d)*U2c(1)*(rhoc(1)*w2c(1)-w2d*rhod))+...

Np(2)*4*pi*Rc(2)^2/(rhod*Omegad)*(w2d*K1c(2)*(m2*w1d*rhod-rhoc(2)*w1c(2))+(1-w2d)*U2c(2)*(rhoc(2)*w2c(2)-w2d*rhod))+...

Np(3)*4*pi*Rc(3)^2/(rhod*Omegad)*(w2d*K1c(3)*(m2*w1d*rhod-rhoc(3)*w1c(3))+(1-w2d)*U2c(3)*(rhoc(3)*w2c(3)-w2d*rhod))+...

Np(4)*4*pi*Rc(4)^2/(rhod*Omegad)*(w2d*K1c(4)*(m2*w1d*rhod-rhoc(4)*w1c(4))+(1-w2d)*U2c(4)*(rhoc(4)*w2c(4)-w2d*rhod))+...

Np(5)*4*pi*Rc(5)^2/(rhod*Omegad)*(w2d*K1c(5)*(m2*w1d*rhod-rhoc(5)*w1c(5))+(1-w2d)*U2c(5)*(rhoc(5)*w2c(5)-w2d*rhod))+...

Np(6)*4*pi*Rc(6)^2/(rhod*Omegad)*(w2d*K1c(6)*(m2*w1d*rhod-rhoc(6)*w1c(6))+(1-w2d)*U2c(6)*(rhoc(6)*w2c(6)-w2d*rhod));

dOmegad=-Omegad*rhodstar*dw2d/rhod+1/rhod*(...

Np(1)*4*pi*Rc(1)^2*(-K1c(1)*(m2*w1d*rhod-w1c(1)*rhoc(1))+U2c(1)*(w2c(1)*rhoc(1)-w2d*rhod))+...

Np(2)*4*pi*Rc(2)^2*(-K1c(2)*(m2*w1d*rhod-w1c(2)*rhoc(2))+U2c(2)*(w2c(2)*rhoc(2)-w2d*rhod))+...

Np(3)*4*pi*Rc(3)^2*(-K1c(3)*(m2*w1d*rhod-w1c(3)*rhoc(3))+U2c(3)*(w2c(3)*rhoc(3)-w2d*rhod))+...

Np(4)*4*pi*Rc(4)^2*(-K1c(4)*(m2*w1d*rhod-w1c(4)*rhoc(4))+U2c(4)*(w2c(4)*rhoc(4)-w2d*rhod))+...

Np(5)*4*pi*Rc(5)^2*(-K1c(5)*(m2*w1d*rhod-w1c(5)*rhoc(5))+U2c(5)*(w2c(5)*rhoc(5)-w2d*rhod))+...

Np(6)*4*pi*Rc(6)^2*(-K1c(6)*(m2*w1d*rhod-w1c(6)*rhoc(6))+U2c(6)*(w2c(6)*rhoc(6)-w2d*rhod));
%%%%%%%%%%%%%%%%%%%%%%%%%%%%%%%%%%%%%%%%%%%%%%%%%%%%%%%%%%%%%%%%%%%%%%%%
%%%%%%%%%%%%%%%%%%%%%%%%%%%%%%%%%%%%%%%%%%%%%%%%%%%%%%%%%%%%%%%%%%%%%%%%

%/////System of ODEs/////
dy(1)=dRa(1); dy(8)=dRa(2); dy(15)=dRa(3); dy(22)=dRa(4); dy(29)=dRa(5);
dy(36)=dRa(6);
dy(2)=dw2b(1); dy(9)=dw2b(2); dy(16)=dw2b(3); dy(23)=dw2b(4); dy(30)=dw2b(5);
dy(37)=dw2b(6);
dy(3)=dRb(1); dy(10)=dRb(2); dy(17)=dRb(3); dy(24)=dRb(4); dy(31)=dRb(5);
dy(38)=dRb(6);
dy(4)=dw2c(1); dy(11)=dw2c(2); dy(18)=dw2c(3); dy(25)=dw2c(4); dy(32)=
dw2c(5); dy(39)=dw2c(6);
dy(5)=dRc(1); dy(12)=dRc(2); dy(19)=dRc(3); dy(26)=dRc(4); dy(33)=dRc(5);
dy(40)=dRc(6);
dy(6)=dw3b(1); dy(13)=dw3b(2); dy(20)=dw3b(3); dy(27)=dw3b(4); dy(34)=dw3b(5);
dy(41)=dw3b(6);
dy(7)=dw4c(1); dy(14)=dw4c(2); dy(21)=dw4c(3); dy(28)=dw4c(4); dy(35)=dw4c(5);

```

```

dy(42)=dw4c(6);

dy(43)=dw2d;
dy(44)=dOmegad;
%%%%%%%%%%%%%%%%%%%%%%%%%%%%%%%%%%%%%%%%%%%%%%%%%%%%%%%%%%%%%%%%%%%%%%%%
end

y0=[Ra0(1),w2b0,Rb0(1),w2c0,Rc0(1),w3b0,w4c0,...
    Ra0(2),w2b0,Rb0(2),w2c0,Rc0(2),w3b0,w4c0,...
    Ra0(3),w2b0,Rb0(3),w2c0,Rc0(3),w3b0,w4c0,...
    Ra0(4),w2b0,Rb0(4),w2c0,Rc0(4),w3b0,w4c0,...
    Ra0(5),w2b0,Rb0(5),w2c0,Rc0(5),w3b0,w4c0,...
    Ra0(6),w2b0,Rb0(6),w2c0,Rc0(6),w3b0,w4c0,...
    w2d0,Omegad0]; %Initial conditions

options=odeset('RelTol',1e-10);
tspan=0:60:TIME;
[t,y] = ode15s(@odesystem,tspan,y0,options); %ODEs solver

%Results
%Domain A
Ra=[y(:,1),y(:,8),y(:,15),y(:,22),y(:,29),y(:,36)];
%Domain B
w2b=[y(:,2),y(:,9),y(:,16),y(:,23),y(:,30),y(:,37)];
w3b=[y(:,6),y(:,13),y(:,20),y(:,27),y(:,34),y(:,41)];
w1b=1-w3b-w2b;
Rb=[y(:,3),y(:,10),y(:,17),y(:,24),y(:,31),y(:,38)];
rhob=(1-w2b-w3b)/rho10+w2b/rho20+w3b/rho30.^(-1);
%Domain C
w2c=[y(:,4),y(:,11),y(:,18),y(:,25),y(:,32),y(:,39)];
w4c=[y(:,7),y(:,14),y(:,21),y(:,28),y(:,35),y(:,42)];
w1c=1-w2c-w4c;
Rc=[y(:,5),y(:,12),y(:,19),y(:,26),y(:,33),y(:,40)];
rhoc=(1-w2c-w4c)/rho10+w2c/rho20+w4c/rho40.^(-1);
%Domain D
w2d=y(:,43);
w1d=1-w2d;
Omegad=y(:,44);
rhod=(1-w2d)/rho10+w2d/rho20.^(-1);
dsfilm=Rc-Rb;
%swelling=(Rc-Rc0)./Rc0*100;

m20=4/3*pi*rhoa*w2a0*(...
    Np(1)*(Ra0(1)^3-R0(1)^3)+...
    Np(2)*(Ra0(2)^3-R0(2)^3)+...
    Np(3)*(Ra0(3)^3-R0(3)^3)+...
    Np(4)*(Ra0(4)^3-R0(4)^3)+...
    Np(5)*(Ra0(5)^3-R0(5)^3)+...
    Np(6)*(Ra0(6)^3-R0(6)^3));

release=w2d.*rhod.*Omegad./m20;

m2a=4/3*pi*rhoa*w2a0*(...
    Np(1)*(Ra(:,1).^3-R0(1).^3)+...
    Np(2)*(Ra(:,2).^3-R0(2).^3)+...
    Np(3)*(Ra(:,3).^3-R0(3).^3)+...
    Np(4)*(Ra(:,4).^3-R0(4).^3)+...
    Np(5)*(Ra(:,5).^3-R0(5).^3)+...
    Np(6)*(Ra(:,6).^3-R0(6).^3));

```

```

m2b=4/3*pi*(...
  Np(1).*w2b(:,1).*rhob(:,1).*(Rb(:,1).^3-Ra(:,1).^3)+...
  Np(2).*w2b(:,2).*rhob(:,2).*(Rb(:,2).^3-Ra(:,2).^3)+...
  Np(3).*w2b(:,3).*rhob(:,3).*(Rb(:,3).^3-Ra(:,3).^3)+...
  Np(4).*w2b(:,4).*rhob(:,4).*(Rb(:,4).^3-Ra(:,4).^3)+...
  Np(5).*w2b(:,5).*rhob(:,5).*(Rb(:,5).^3-Ra(:,5).^3)+...
  Np(6).*w2b(:,6).*rhob(:,6).*(Rb(:,6).^3-Ra(:,6).^3));

m2c=4/3*pi*(...
  Np(1)*w2c(:,1).*rhoc(:,1).*(Rc(:,1).^3-Rb(:,1).^3)+...
  Np(2)*w2c(:,2).*rhoc(:,2).*(Rc(:,2).^3-Rb(:,2).^3)+...
  Np(3)*w2c(:,3).*rhoc(:,3).*(Rc(:,3).^3-Rb(:,3).^3)+...
  Np(4)*w2c(:,4).*rhoc(:,4).*(Rc(:,4).^3-Rb(:,4).^3)+...
  Np(5)*w2c(:,5).*rhoc(:,5).*(Rc(:,5).^3-Rb(:,5).^3)+...
  Np(6)*w2c(:,6).*rhoc(:,6).*(Rc(:,6).^3-Rb(:,6).^3));

%//////////Release from the ith%class//////////
m201=4/3*pi*rhoa*w2a0*(Np(1)*(Ra0(1)^3-R0(1)^3));
m2a1=4/3.*pi.*rhoa.*w2a0.*(Np(1)*(Ra(:,1).^3-R0(1).^3));
m2b1=4/3*pi*(Np(1).*w2b(:,1).*rhob(:,1).*(Rb(:,1).^3-Ra(:,1).^3));
m2c1=4/3*pi*(Np(1)*w2c(:,1).*rhoc(:,1).*(Rc(:,1).^3-Rb(:,1).^3));
release1=(m201-(m2a1+m2b1+m2c1))/m201;

m202=4/3*pi*rhoa*w2a0*(Np(2)*(Ra0(2)^3-R0(2)^3));
m2a2=4/3*pi*rhoa*w2a0*(Np(2)*(Ra(:,2).^3-R0(2).^3));
m2b2=4/3*pi*(Np(2).*w2b(:,2).*rhob(:,2).*(Rb(:,2).^3-Ra(:,2).^3));
m2c2=4/3*pi*(Np(2)*w2c(:,2).*rhoc(:,2).*(Rc(:,2).^3-Rb(:,2).^3));
release2=(m202-(m2a2+m2b2+m2c2))/m202;

m203=4/3*pi*rhoa*w2a0*(Np(3)*(Ra0(3)^3-R0(3)^3));
m2a3=4/3*pi*rhoa*w2a0*(Np(3)*(Ra(:,3).^3-R0(3).^3));
m2b3=4/3*pi*(Np(3).*w2b(:,3).*rhob(:,3).*(Rb(:,3).^3-Ra(:,3).^3));
m2c3=4/3*pi*(Np(3)*w2c(:,3).*rhoc(:,3).*(Rc(:,3).^3-Rb(:,3).^3));
release3=(m203-(m2a3+m2b3+m2c3))/m203;

m204=4/3*pi*rhoa*w2a0*(Np(4)*(Ra0(4)^3-R0(4)^3));
m2a4=4/3*pi*rhoa*w2a0*(Np(4)*(Ra(:,4).^3-R0(4).^3));
m2b4=4/3*pi*(Np(4).*w2b(:,4).*rhob(:,4).*(Rb(:,4).^3-Ra(:,4).^3));
m2c4=4/3*pi*(Np(4)*w2c(:,4).*rhoc(:,4).*(Rc(:,4).^3-Rb(:,4).^3));
release4=(m204-(m2a4+m2b4+m2c4))/m204;

m205=4/3*pi*rhoa*w2a0*(Np(5)*(Ra0(5)^3-R0(5)^3));
m2a5=4/3*pi*rhoa*w2a0*(Np(5)*(Ra(:,5).^3-R0(5).^3));
m2b5=4/3*pi*(Np(5).*w2b(:,5).*rhob(:,5).*(Rb(:,5).^3-Ra(:,5).^3));
m2c5=4/3*pi*(Np(5)*w2c(:,5).*rhoc(:,5).*(Rc(:,5).^3-Rb(:,5).^3));
release5=(m205-(m2a5+m2b5+m2c5))/m205;

m206=4/3*pi*rhoa*w2a0*(Np(6)*(Ra0(6)^3-R0(6)^3));
m2a6=4/3*pi*rhoa*w2a0*(Np(6)*(Ra(:,6).^3-R0(6).^3));
m2b6=4/3*pi*(Np(6).*w2b(:,6).*rhob(:,6).*(Rb(:,6).^3-Ra(:,6).^3));
m2c6=4/3*pi*(Np(6)*w2c(:,6).*rhoc(:,6).*(Rc(:,6).^3-Rb(:,6).^3));
release6=(m206-(m2a6+m2b6+m2c6))/m206;
%//////////End Release from the ith class//////////

%//////////Figures//////////

figure
plot(t/3600,Ra*10^6,'-',t/3600,Rb*10^6,'--',t/3600,Rc*10^6,'.')
title('Radii evolution')
xlabel('Time [h]')

```

```
ylabel('Radius [um]')
legend('Ra', 'Rb', 'Rc')
```

```
figure
plot(t/3600,w2b,t/3600,w2c)
title('Drug fractions')
xlabel('Time [h]')
ylabel('Mass fraction [-]')
legend('w2b', 'w2c')
```

```
figure
plot(t/3600,release,'-',t/3600,release1,'-',t/3600,release2,'-',t/3600,release3,'-',t/3600,release4,'-',t/3600,release5,'-',t/3600,release6,'-')
title('Release from the ith classes')
xlabel('Time [h]')
ylabel('Release [-]')
legend('release TOT', 'release I', 'release II', 'release III', 'release IV', 'release V', 'release VI')
```

```
% %/////Experimental data////////////////////////////////////
```

```
texp=[0.016666667,0.5,1,1.5,2,3,4,5,6,7,9,11,13,15,17,19,21,23,25,27,29,32,33,35,37,39,41,43,45,47,49,51,53,55,57,59,61,63,65,67,69,71,73,75,77];
```

```
y20=[1.90240316,6.488009571,10.08250555,14.05554622,18.29947852,25.96874285,33.43354749,40.61199147,47.65716631,54.01040045,66.1672172,75.91891377,82.43046676,87.50249762,91.68557423,92.94562351,96.34256413,92.04639665,98.43055252,100.7490821,99.97138893,100.1995253,101.4802649,99.89193702,98.99139666,100.8077398,100,100,100,100,100,100,100,100,100,100,100,100,100,100,100,100,100,100,100,100]; %Global TP release with film thickness of 20 um
```

```
y30=[1.310134018,5.100524125,7.501053805,10.1312529,13.43881706,17.69370403,22.73221795,27.66044764,32.35499387,36.98307846,46.18394602,55.09346624,62.83360535,69.7154417,75.46837038,78.27760034,86.41201019,89.42124639,92.19890086,95.74649776,95.51165956,99.26835398,99.19284621,101.168998,99.65818819,99.9796757,100,100,100,100,100,100,100,100,100,100,100,100,100,100,100,100,100,100,100,100];
```

```
y60=[1.981569582,5.115953377,6.765312431,8.137103313,9.353900156,11.22879192,13.79075693,16.71703661,18.902185,21.61699951,26.00686318,30.75278334,35.28025299,39.22761513,43.25815544,47.05651527,50.97411896,55.24559284,58.80588289,62.18060217,65.82993692,68.66016577,71.95850492,74.53939,76.75124643,78.92388318,82.16850129,84.34895295,85.95549981,87.87383053,89.39914511,90.28398997,90.62647986,92.40681804,93.39578489,94.66340375,94.54008634,96.17876151,96.59720818,97.49118014,97.11047724,97.55955686,98.22587734,99.96597617,98.83363928]; %Global TP release with film thickness of 60 um
```

```
% %/////End Experimental data////////////////////////////////////
```

```
figure
plot(texp,y20,'o',texp,y30,'+',texp,y60,'x',t/3600,release*100,'-');
xlabel('Time [h]');
ylabel('Release %');
legend('Exp 20um', 'Exp 30um', 'Exp 60um', 'Mod 20um')
```

```
%////////////////////////////////////End Figures////////////////////////////////////
```

```
end
```

```

%Everything is in SI units"

function Whole_dose_Film_thickness

%//////////Assign a film thickness with a normal distribution//////////
mu=13.3E-6;
sigma=5E-6;
pd = makedist('Normal','mu',mu,'sigma',sigma);
upper=mu*3;
x=linspace(0,upper,11);
for j=1:10
    filmt(j)=(x(j)+x(j+1))/2;
end
z = cdf(pd,x);
for i=2:11
    ni_on_ntot(i-1)=(z(i)-z(i-1));
end
plot(x,z)
%//////////End Assign a film thickness with a normal distribution//////////

%//////////Parameters//////////

%Initial geometry
R0=[300E-6,300E-6,300E-6,300E-6,300E-6,300E-6,300E-6,300E-6,300E-6,300E-6];
Rb0=R0+6.3E-6;
Ra0=Rb0-1E-8;
Rc0=Rb0+filmt;
Ntot=5000; %Total Number of pellets
Np=ni_on_ntot*Ntot; %Number of pellets in each class

%Dissolution Time [s]
TIME=80*3600;
%Densities [kg/m^3]
rho10=1000; rho20=1200; rho30=1200; rho40=1200;

%Diffusivities [m^2/s]
D2b=1.5E-10; % from doi:10.1016/j.ijpharm.2015.03.054
D1b=2.2E-9; % from doi:10.1016/j.ijpharm.2015.03.054
D2c=3.2E-13; % from Kazlauske et al. (submitted)
D1c=1.99E-12; % from Kazlauske et al. (submitted)
D2d=8.21E-10; % from doi:10.1016/S0168-3659(01)00424-2
D1self=3E-9; % from doi:10.1039/B005319H
%See the Transport coefficients definition

%Initial mass fractions
%Domain A
w2sat=0.0115; % from doi:10.1002/jps.26007402091
w2a0=0.9; w3a0=1-w2a0;
%Domain B
w2b0=0;
w3b0=0;
%Domain C
w4c0=1;
w2c0=0;
rhoc0=(1-w2c0-w4c0)/rho10+w2c0/rho20+w4c0/rho40)^(-1);
%Domain D
w2d0=0; %w1d0=1-w2d0;

Omegad0=1E-3; % Initial dissolution medium [m^3]

```

```

%//////////End Parameters//////////
function dy = odesystem (t,y)
dy=zeros(72,1); %Initialization
Ra= [y(1),y(8), y(15),y(22),y(29),y(36),y(43),y(50),y(57),y(64)];
w2b=[y(2),y(9), y(16),y(23),y(30),y(37),y(44),y(51),y(58),y(65)];
Rb= [y(3),y(10),y(17),y(24),y(31),y(38),y(45),y(52),y(59),y(66)];
w2c=[y(4),y(11),y(18),y(25),y(32),y(39),y(46),y(53),y(60),y(67)];
Rc= [y(5),y(12),y(19),y(26),y(33),y(40),y(47),y(54),y(61),y(68)];
w3b=[y(6),y(13),y(20),y(27),y(34),y(41),y(48),y(55),y(62),y(69)];
w4c=[y(7),y(14),y(21),y(28),y(35),y(42),y(49),y(56),y(63),y(70)];
w2d=y(71);
Omegad=y(72);

rhoa=(w2a0/rho20+w3a0/rho30)^(-1); %Density of domain A OK
rhub=((1-w2b-w3b)/rho10+w2b/rho20+w3b/rho30).^(-1); %Density of domain B
OK
rhoc=((1-w2c-w4c)/rho10+w2c/rho20+w4c/rho40).^(-1); %Density of domain C
OK
rhod=((1-w2d)/rho10+w2d/rho20).^(-1); %Density of domain D OK
w1b=1-w2b-w3b; %OK
w1c=1-w2c-w4c; %OK
w1d=1-w2d; %OK

%////Stop condition when Ra reach R0 or when there is not enough
water/////
w2bStar=w2b./(w1b+w2b);
kdiss0=D2b./Ra;
kdiss=[0,0,0,0,0,0,0,0,0,0]; %initialization kdiss

if Ra(1)>R0(1) && (w2sat-w2bStar(1))>0
    kdiss(1)=kdiss0(1);
else
    kdiss(1)=0;
end

if Ra(2)>R0(2) && (w2sat-w2bStar(2))>0
    kdiss(2)=kdiss0(2);
else
    kdiss(2)=0;
end

if Ra(3)>R0(3) && (w2sat-w2bStar(3))>0
    kdiss(3)=kdiss0(3);
else
    kdiss(3)=0;
end

if Ra(4)>R0(4) && (w2sat-w2bStar(4))>0
    kdiss(4)=kdiss0(4);
else
    kdiss(4)=0;
end

if Ra(5)>R0(5) && (w2sat-w2bStar(5))>0
    kdiss(5)=kdiss0(5);
else
    kdiss(5)=0;
end

```

```

if Ra(6)>R0(6) && (w2sat-w2bStar(6))>0
    kdiss(6)=kdiss0(6);
else
    kdiss(6)=0;
end
if Ra(7)>R0(7) && (w2sat-w2bStar(7))>0
    kdiss(7)=kdiss0(7);
else
    kdiss(7)=0;
end
if Ra(8)>R0(8) && (w2sat-w2bStar(8))>0
    kdiss(8)=kdiss0(8);
else
    kdiss(8)=0;
end
if Ra(9)>R0(9) && (w2sat-w2bStar(9))>0
    kdiss(9)=kdiss0(9);
else
    kdiss(9)=0;
end
if Ra(10)>R0(10) && (w2sat-w2bStar(10))>0
    kdiss(10)=kdiss0(10);
else
    kdiss(10)=0;
end
%////End Stop condition when Ra reach R0 or when there is not enough
water/

%//////////Transport
coefficients//////////
k2b=D2b./(Rb-Ra);
k2c=D2c./(Rc-Rb);
k2d=D2d./Rc;
U2b=(1./(k2b)+1./(k2c)).^(-1);
U2c=(1./(k2c)+1./(k2d)).^(-1);
k1b=D1b./(Rb-Ra);
k1c=D1c./(Rc-Rb);
m1=4.95; %w1b=m1*w1c
U1b=(1./(k1b)+m1./(k1c)).^(-1);
k1d=D1self./Rc;
m2=0.2; %w1c=m2*w1d
K1c=(1./(k1c)+m2./(k1d)).^(-1);
%//////////End Transport
coefficients//////////

%//////////Parameters defined during the ODEs
rearrangement//////////
rho2b3=rho10.*rho20-rho20.*rho30; %OK
rho2b2=rho10.*rho30-rho20.*rho30; %OK

rhostar=(rho20.*rho30.*(1-w2b-w3b)+rho10.*rho30.*w2b+rho10.*rho20.*w3b).^2./
(rho10.*rho20.*rho30); %OK
alfa=w3b.*(rho2b2./rhostar)./(rhob-w3b.*rho2b3./rhostar); %OK
beta=-rhob.*w3b.*3.*Rb.^2./((Rb.^3-Ra.^3).*(rhob-w3b.*rho2b3./rhostar));
%OK
gamma=rhob.*w3b.*3.*Ra.^2./((Rb.^3-Ra.^3).*(rhob-w3b.*rho2b3./rhostar));
%OK

delta=3.*Ra.^2.*rhob.*kdiss.*w3a0.*(w2sat-w2bStar)./(w2a0.*(Rb.^3-Ra.^3).*(rhob-w3b.*rho2b3./rhostar)); %OK

```

```

lambda=3.*Rb.^2.*rhob-(Rb.^3-Ra.^3).*beta.*rho2b3./rhostar; %OK
chsi=3.*Ra.^2.*rhob+gamma.*(Rb.^3-Ra.^3).*rho2b3./rhostar; %OK
eps=rho2b2./rhostar.*(Rb.^3-Ra.^3)+rho2b3.*alfa.*(Rb.^3-Ra.^3)./rhostar;
%OK

zeta=(Rb.^3-Ra.^3).*rho2b3.*delta./rhostar+3.*Rb.^2.*U1b.*(m1.*w1c.*rhoc-w1b.*
rhob)-3.*Rb.^2.*U2b.*(w2b.*rhob-w2c.*rhoc)+3.*Ra.^2.*kdiss.*rhob.*(w2sat-w2b
Star)./w2a0; %OK

fi=rhob.*(Rb.^3-Ra.^3)-w2b.*(Rb.^3-Ra.^3).*(rho2b2./rhostar+rho2b3.*alfa./rho
star)+eps./lambda.*(rhob.*w2b.*3.*Rb.^2-w2b.*(Rb.^3-Ra.^3).*beta.*rho2b3./rho
star); %OK

eta=-(-rhob.*w2b.*3.*Ra.^2-w2b.*(Rb.^3-Ra.^3).*rho2b3.*gamma./rhostar+chsi./l
ambda.*(rhob.*w2b.*3.*Rb.^2-w2b.*(Rb.^3-Ra.^3).*rho2b3.*beta./rhostar)); %OK

tau=-zeta./lambda.*(rhob.*w2b.*3.*Rb.^2-w2b.*(Rb.^3-Ra.^3).*rho2b3.*beta./rho
star)+w2b.*(Rb.^3-Ra.^3).*rho2b3.*delta./rhostar+3.*Ra.^2.*kdiss.*rhob.*(w2sa
t-w2bStar)-3.*Rb.^2.*U2b.*(w2b.*rhob-w2c.*rhoc); %OK
a=rho40.*(rho10-rho20); %OK
b=rho20.*(rho10-rho40); %OK

rhocstar=(rho20.*rho40.*(1-w2c-w4c)+rho10.*rho40.*w2c+rho10.*rho20.*w4c).^2./
(rho10.*rho20.*rho40); %OK
A1=rhoc.*(Rc.^3-Rb.^3)-b.*w4c.*(Rc.^3-Rb.^3)./rhocstar; %OK
B1=-rhoc.*w4c.*3.*Rc.^2; %OK
C1=3.*Rb.^2.*rhoc.*w4c./lambda.*(chsi+eps.*eta./fi); %OK
D1=a.*w4c.*(Rc.^3-Rb.^3)./rhocstar; %OK
E1=3.*Rb.^2.*rhoc.*w4c./lambda.*(eps.*tau./fi+zeta); %OK
F1=3.*rhoc.*Rc.^2-(Rc.^3-Rb.^3).*b.*B1./(rhocstar.*A1); %OK

G1=rhoc.*3.*Rb.^2.*(chsi./lambda+eps.*eta./(lambda.*fi))+(Rc.^3-Rb.^3).*b.*C1
./ (rhocstar.*A1); %OK
H1=(Rc.^3-Rb.^3).*(b.*D1./(rhocstar.*A1)+a./rhocstar); %OK

I1=(Rc.^3-Rb.^3).*b.*E1./(rhocstar.*A1)+3.*Rc.^2.*K1c.*(m2.*w1d.*rhod-w1c.*rh
oc)-3.*Rb.^2.*U1b.*(m1.*w1c.*rhoc-w1b.*rhob)+3.*Rb.^2.*U2b.*(w2b.*rhob-w2c.*r
hoc)-3.*Rc.^2.*U2c.*(w2c.*rhoc-w2d.*rhod)+rhoc.*3.*Rb.^2.*(eps.*tau./(lambda.
*fi)+zeta./lambda); %OK

L1=rhoc.*w2c.*3.*Rc.^2.*H1./F1+rhoc.*(Rc.^3-Rb.^3)+w2c.*(Rc.^3-Rb.^3).*(-a./r
hocstar-b.*(D1+B1.*H1./F1))/(rhocstar.*A1); %OK

M1=- (rhoc.*w2c.*(3.*Rc.^2.*G1./F1-3.*Rb.^2.*chsi./lambda-3.*Rb.^2.*eta.*eps./
(lambda.*fi))-w2c.*(Rc.^3-Rb.^3).*b.*(C1+B1.*G1./F1))/(rhocstar.*A1); %OK

N1=-rhoc.*w2c.*(3.*Rc.^2.*I1./F1-3.*Rb.^2.*(zeta+eta.*tau./fi)./lambda)+w2c.*
(Rc.^3-Rb.^3).*b./(rhocstar.*A1).*(E1+B1.*I1./F1)+3.*Rb.^2.*U2b.*(w2b.*rhob-w
2c.*rhoc)-3.*Rc.^2.*U2c.*(w2c.*rhoc-w2d.*rhod); %OK
rhodstar=rho10.*rho20.*(rho20-rho10)/(rho20.*(1-w2d)+rho10.*w2d).^2; %OK

dRa=-kdiss.*rhob./(rhoa.*w2a0).*(w2sat-w2bStar); %OK
dw2b=(eta.*dRa+tau)./fi; %OK
dRb=(chsi.*dRa+eps.*dw2b+zeta)./lambda; %OK
dw3b=alfa.*dw2b+beta.*dRb+gamma.*dRa+delta; %OK
dw2c=(M1.*dRa+N1)./L1; %OK
dRc=(G1.*dRa+H1.*dw2c+I1)./F1; %OK
dw4c=(B1.*dRc+C1.*dRa+D1.*dw2c+E1)./A1; %OK
dw2d= ...

```

$$Np(1) * 4 * \pi * Rc(1) ^ 2 / (rhod * Omegad) * (w2d * K1c(1) * (m2 * w1d * rhod - rhoc(1) * w1c(1)) + (1 - w2d) * U2c(1) * (rhoc(1) * w2c(1) - w2d * rhod)) + \dots$$

$$Np(2) * 4 * \pi * Rc(2) ^ 2 / (rhod * Omegad) * (w2d * K1c(2) * (m2 * w1d * rhod - rhoc(2) * w1c(2)) + (1 - w2d) * U2c(2) * (rhoc(2) * w2c(2) - w2d * rhod)) + \dots$$

$$Np(3) * 4 * \pi * Rc(3) ^ 2 / (rhod * Omegad) * (w2d * K1c(3) * (m2 * w1d * rhod - rhoc(3) * w1c(3)) + (1 - w2d) * U2c(3) * (rhoc(3) * w2c(3) - w2d * rhod)) + \dots$$

$$Np(4) * 4 * \pi * Rc(4) ^ 2 / (rhod * Omegad) * (w2d * K1c(4) * (m2 * w1d * rhod - rhoc(4) * w1c(4)) + (1 - w2d) * U2c(4) * (rhoc(4) * w2c(4) - w2d * rhod)) + \dots$$

$$Np(5) * 4 * \pi * Rc(5) ^ 2 / (rhod * Omegad) * (w2d * K1c(5) * (m2 * w1d * rhod - rhoc(5) * w1c(5)) + (1 - w2d) * U2c(5) * (rhoc(5) * w2c(5) - w2d * rhod)) + \dots$$

$$Np(6) * 4 * \pi * Rc(6) ^ 2 / (rhod * Omegad) * (w2d * K1c(6) * (m2 * w1d * rhod - rhoc(6) * w1c(6)) + (1 - w2d) * U2c(6) * (rhoc(6) * w2c(6) - w2d * rhod)) + \dots$$

$$Np(7) * 4 * \pi * Rc(7) ^ 2 / (rhod * Omegad) * (w2d * K1c(7) * (m2 * w1d * rhod - rhoc(7) * w1c(7)) + (1 - w2d) * U2c(7) * (rhoc(7) * w2c(7) - w2d * rhod)) + \dots$$

$$Np(8) * 4 * \pi * Rc(8) ^ 2 / (rhod * Omegad) * (w2d * K1c(8) * (m2 * w1d * rhod - rhoc(8) * w1c(8)) + (1 - w2d) * U2c(8) * (rhoc(8) * w2c(8) - w2d * rhod)) + \dots$$

$$Np(9) * 4 * \pi * Rc(9) ^ 2 / (rhod * Omegad) * (w2d * K1c(9) * (m2 * w1d * rhod - rhoc(9) * w1c(9)) + (1 - w2d) * U2c(9) * (rhoc(9) * w2c(9) - w2d * rhod)) + \dots$$

$$Np(10) * 4 * \pi * Rc(10) ^ 2 / (rhod * Omegad) * (w2d * K1c(10) * (m2 * w1d * rhod - rhoc(10) * w1c(10)) + (1 - w2d) * U2c(10) * (rhoc(10) * w2c(10) - w2d * rhod));$$

$$dOmegad = -Omegad * rhodstar * dw2d / rhod + 1 / rhod * (\dots$$

$$Np(1) * 4 * \pi * Rc(1) ^ 2 * (-K1c(1) * (m2 * w1d * rhod - w1c(1) * rhoc(1)) + U2c(1) * (w2c(1) * rhoc(1) - w2d * rhod)) + \dots$$

$$Np(2) * 4 * \pi * Rc(2) ^ 2 * (-K1c(2) * (m2 * w1d * rhod - w1c(2) * rhoc(2)) + U2c(2) * (w2c(2) * rhoc(2) - w2d * rhod)) + \dots$$

$$Np(3) * 4 * \pi * Rc(3) ^ 2 * (-K1c(3) * (m2 * w1d * rhod - w1c(3) * rhoc(3)) + U2c(3) * (w2c(3) * rhoc(3) - w2d * rhod)) + \dots$$

$$Np(4) * 4 * \pi * Rc(4) ^ 2 * (-K1c(4) * (m2 * w1d * rhod - w1c(4) * rhoc(4)) + U2c(4) * (w2c(4) * rhoc(4) - w2d * rhod)) + \dots$$

$$Np(5) * 4 * \pi * Rc(5) ^ 2 * (-K1c(5) * (m2 * w1d * rhod - w1c(5) * rhoc(5)) + U2c(5) * (w2c(5) * rhoc(5) - w2d * rhod)) + \dots$$

$$Np(6) * 4 * \pi * Rc(6) ^ 2 * (-K1c(6) * (m2 * w1d * rhod - w1c(6) * rhoc(6)) + U2c(6) * (w2c(6) * rhoc(6) - w2d * rhod)) + \dots$$

$$Np(7) * 4 * \pi * Rc(7) ^ 2 * (-K1c(7) * (m2 * w1d * rhod - w1c(7) * rhoc(7)) + U2c(7) * (w2c(7) * rhoc(7) - w2d * rhod)) + \dots$$

$$Np(8) * 4 * \pi * Rc(8) ^ 2 * (-K1c(8) * (m2 * w1d * rhod - w1c(8) * rhoc(8)) + U2c(8) * (w2c(8) * rhoc(8) - w2d * rhod)) + \dots$$

$$Np(9) * 4 * \pi * Rc(9) ^ 2 * (-K1c(9) * (m2 * w1d * rhod - w1c(9) * rhoc(9)) + U2c(9) * (w2c(9) * rhoc(9) - w2d * rhod)) + \dots$$

```

Np(10)*4*pi*Rc(10)^2*(-K1c(10)*(m2*w1d*rhod-w1c(10)*rhoc(10))+U2c(10)*(w2c(10)
)*rhoc(10)-w2d*rhod));
%//////////End Parameters defined during the ODEs
rearrangement//////////

%//////////System of ODEs//////////
dy(1)=dRa(1); dy(8)=dRa(2); dy(15)=dRa(3); dy(22)=dRa(4); dy(29)=dRa(5);
dy(36)=dRa(6); dy(43)=dRa(7); dy(50)=dRa(8); dy(57)=dRa(9);
dy(64)=dRa(10);
dy(2)=dw2b(1); dy(9)=dw2b(2); dy(16)=dw2b(3); dy(23)=dw2b(4); dy(30)=dw2b(5);
dy(37)=dw2b(6); dy(44)=dw2b(7); dy(51)=dw2b(8); dy(58)=dw2b(9);
dy(65)=dw2b(10);
dy(3)=dRb(1); dy(10)=dRb(2); dy(17)=dRb(3); dy(24)=dRb(4); dy(31)=dRb(5);
dy(38)=dRb(6); dy(45)=dRb(7); dy(52)=dRb(8); dy(59)=dRb(9);
dy(66)=dRb(10);
dy(4)=dw2c(1); dy(11)=dw2c(2); dy(18)=dw2c(3); dy(25)=dw2c(4); dy(32)=dw2c(5);
dy(39)=dw2c(6); dy(46)=dw2c(7); dy(53)=dw2c(8); dy(60)=dw2c(9);
dy(67)=dw2c(10);
dy(5)=dRc(1); dy(12)=dRc(2); dy(19)=dRc(3); dy(26)=dRc(4); dy(33)=dRc(5);
dy(40)=dRc(6); dy(47)=dRc(7); dy(54)=dRc(8); dy(61)=dRc(9);
dy(68)=dRc(10);
dy(6)=dw3b(1); dy(13)=dw3b(2); dy(20)=dw3b(3); dy(27)=dw3b(4); dy(34)=dw3b(5);
dy(41)=dw3b(6); dy(48)=dw3b(7); dy(55)=dw3b(8); dy(62)=dw3b(9);
dy(69)=dw3b(10);
dy(7)=dw4c(1); dy(14)=dw4c(2); dy(21)=dw4c(3); dy(28)=dw4c(4); dy(35)=dw4c(5);
dy(42)=dw4c(6); dy(49)=dw4c(7); dy(56)=dw4c(8); dy(63)=dw4c(9);
dy(70)=dw4c(10);

dy(71)=dw2d;
dy(72)=dOmegad;
%//////////End System of ODEs//////////
end

y0=[Ra0(1),w2b0,Rb0(1),w2c0,Rc0(1),w3b0,w4c0,...
Ra0(2),w2b0,Rb0(2),w2c0,Rc0(2),w3b0,w4c0,...
Ra0(3),w2b0,Rb0(3),w2c0,Rc0(3),w3b0,w4c0,...
Ra0(4),w2b0,Rb0(4),w2c0,Rc0(4),w3b0,w4c0,...
Ra0(5),w2b0,Rb0(5),w2c0,Rc0(5),w3b0,w4c0,...
Ra0(6),w2b0,Rb0(6),w2c0,Rc0(6),w3b0,w4c0,...
Ra0(7),w2b0,Rb0(7),w2c0,Rc0(7),w3b0,w4c0,...
Ra0(8),w2b0,Rb0(8),w2c0,Rc0(8),w3b0,w4c0,...
Ra0(9),w2b0,Rb0(9),w2c0,Rc0(9),w3b0,w4c0,...
Ra0(10),w2b0,Rb0(10),w2c0,Rc0(10),w3b0,w4c0,...
w2d0,Omegad0]; %Initial conditions

options=odeset('RelTol',1e-10);
tspan=0:60:TIME;
[t,y] = odel5s(@odesystem,tspan,y0,options); %ODEs solver

%Results
%Domain A
Ra=[y(:,1),y(:,8),y(:,15),y(:,22),y(:,29),y(:,36),y(:,43),y(:,50),y(:,57),y(
,64)];
%Domain B
w2b=[y(:,2),y(:,9),y(:,16),y(:,23),y(:,30),y(:,37),y(:,44),y(:,51),y(:,58),y(
:,65)];
w3b=[y(:,6),y(:,13),y(:,20),y(:,27),y(:,34),y(:,41),y(:,48),y(:,55),y(:,62),y(
(:,69)];
w1b=1-w3b-w2b;
Rb=[y(:,3),y(:,10),y(:,17),y(:,24),y(:,31),y(:,38),y(:,45),y(:,52),y(:,59),y(

```

```

:, 66)];
rhob = ( (1-w2b-w3b) / rho10+w2b/rho20+w3b/rho30) .^ (-1);
%Domain C
w2c = [y(:, 4), y(:, 11), y(:, 18), y(:, 25), y(:, 32), y(:, 39), y(:, 46), y(:, 53), y(:, 60), y
(:, 67)];
w4c = [y(:, 7), y(:, 14), y(:, 21), y(:, 28), y(:, 35), y(:, 42), y(:, 49), y(:, 56), y(:, 63), y
(:, 70)];
w1c = 1-w2c-w4c;
Rc = [y(:, 5), y(:, 12), y(:, 19), y(:, 26), y(:, 33), y(:, 40), y(:, 47), y(:, 54), y(:, 61), y(
(:, 68)];
rhoc = ( (1-w2c-w4c) / rho10+w2c/rho20+w4c/rho40) .^ (-1);
%Domain D
w2d = y(:, 71);
w1d = 1-w2d;
Omegad = y(:, 72);
rhod = ( (1-w2d) / rho10+w2d/rho20) .^ (-1);
dsfilm = Rc - Rb;
%swelling = (Rc - Rc0) ./ Rc0 * 100;

m20 = 4/3*pi*rhoa*w2a0*(...
    Np(1) * (Ra0(1)^3 - R0(1)^3) + ...
    Np(2) * (Ra0(2)^3 - R0(2)^3) + ...
    Np(3) * (Ra0(3)^3 - R0(3)^3) + ...
    Np(4) * (Ra0(4)^3 - R0(4)^3) + ...
    Np(5) * (Ra0(5)^3 - R0(5)^3) + ...
    Np(6) * (Ra0(6)^3 - R0(6)^3) + ...
    Np(7) * (Ra0(7)^3 - R0(7)^3) + ...
    Np(8) * (Ra0(8)^3 - R0(8)^3) + ...
    Np(9) * (Ra0(9)^3 - R0(9)^3) + ...
    Np(10) * (Ra0(10)^3 - R0(10)^3);

release = w2d.*rhod.*Omegad./m20;

m2a = 4/3*pi*rhoa*w2a0*(...
    Np(1) * (Ra(:, 1).^3 - R0(1).^3) + ...
    Np(2) * (Ra(:, 2).^3 - R0(2).^3) + ...
    Np(3) * (Ra(:, 3).^3 - R0(3).^3) + ...
    Np(4) * (Ra(:, 4).^3 - R0(4).^3) + ...
    Np(5) * (Ra(:, 5).^3 - R0(5).^3) + ...
    Np(6) * (Ra(:, 6).^3 - R0(6).^3) + ...
    Np(7) * (Ra(:, 7).^3 - R0(7).^3) + ...
    Np(8) * (Ra(:, 8).^3 - R0(8).^3) + ...
    Np(9) * (Ra(:, 9).^3 - R0(9).^3) + ...
    Np(10) * (Ra(:, 10).^3 - R0(10).^3);

m2b = 4/3*pi*(...
    Np(1) .* w2b(:, 1) .* rhob(:, 1) .* (Rb(:, 1).^3 - Ra(:, 1).^3) + ...
    Np(2) .* w2b(:, 2) .* rhob(:, 2) .* (Rb(:, 2).^3 - Ra(:, 2).^3) + ...
    Np(3) .* w2b(:, 3) .* rhob(:, 3) .* (Rb(:, 3).^3 - Ra(:, 3).^3) + ...
    Np(4) .* w2b(:, 4) .* rhob(:, 4) .* (Rb(:, 4).^3 - Ra(:, 4).^3) + ...
    Np(5) .* w2b(:, 5) .* rhob(:, 5) .* (Rb(:, 5).^3 - Ra(:, 5).^3) + ...
    Np(6) .* w2b(:, 6) .* rhob(:, 6) .* (Rb(:, 6).^3 - Ra(:, 6).^3) + ...
    Np(7) .* w2b(:, 7) .* rhob(:, 7) .* (Rb(:, 7).^3 - Ra(:, 7).^3) + ...
    Np(8) .* w2b(:, 8) .* rhob(:, 8) .* (Rb(:, 8).^3 - Ra(:, 8).^3) + ...
    Np(9) .* w2b(:, 9) .* rhob(:, 9) .* (Rb(:, 9).^3 - Ra(:, 9).^3) + ...
    Np(10) .* w2b(:, 10) .* rhob(:, 10) .* (Rb(:, 10).^3 - Ra(:, 10).^3);

m2c = 4/3*pi*(...
    Np(1) * w2c(:, 1) .* rhoc(:, 1) .* (Rc(:, 1).^3 - Rb(:, 1).^3) + ...

```

```

Np(2)*w2c(:,2).*rhoc(:,2).*(Rc(:,2).^3-Rb(:,2).^3)+...
Np(3)*w2c(:,3).*rhoc(:,3).*(Rc(:,3).^3-Rb(:,3).^3)+...
Np(4)*w2c(:,4).*rhoc(:,4).*(Rc(:,4).^3-Rb(:,4).^3)+...
Np(5)*w2c(:,5).*rhoc(:,5).*(Rc(:,5).^3-Rb(:,5).^3)+...
Np(6)*w2c(:,6).*rhoc(:,6).*(Rc(:,6).^3-Rb(:,6).^3)+...
Np(7)*w2c(:,7).*rhoc(:,7).*(Rc(:,7).^3-Rb(:,7).^3)+...
Np(8)*w2c(:,8).*rhoc(:,8).*(Rc(:,8).^3-Rb(:,8).^3)+...
Np(9)*w2c(:,9).*rhoc(:,9).*(Rc(:,9).^3-Rb(:,9).^3)+...
Np(10)*w2c(:,10).*rhoc(:,10).*(Rc(:,10).^3-Rb(:,10).^3));

%//////////Release from the ith class//////////
m201=4/3*pi*rhoa*w2a0*(Np(1)*(Ra0(1)^3-R0(1)^3));
m2a1=4/3.*pi.*rhoa.*w2a0.*(Np(1)*(Ra(:,1).^3-R0(1).^3));
m2b1=4/3*pi*(Np(1).*w2b(:,1).*rhob(:,1).*(Rb(:,1).^3-Ra(:,1).^3));
m2c1=4/3*pi*(Np(1)*w2c(:,1).*rhoc(:,1).*(Rc(:,1).^3-Rb(:,1).^3));
release1=(m201-(m2a1+m2b1+m2c1))/m201;

m202=4/3*pi*rhoa*w2a0*(Np(2)*(Ra0(2)^3-R0(2)^3));
m2a2=4/3*pi*rhoa*w2a0*(Np(2)*(Ra(:,2).^3-R0(2).^3));
m2b2=4/3*pi*(Np(2).*w2b(:,2).*rhob(:,2).*(Rb(:,2).^3-Ra(:,2).^3));
m2c2=4/3*pi*(Np(2)*w2c(:,2).*rhoc(:,2).*(Rc(:,2).^3-Rb(:,2).^3));
release2=(m202-(m2a2+m2b2+m2c2))/m202;

m203=4/3*pi*rhoa*w2a0*(Np(3)*(Ra0(3)^3-R0(3)^3));
m2a3=4/3*pi*rhoa*w2a0*(Np(3)*(Ra(:,3).^3-R0(3).^3));
m2b3=4/3*pi*(Np(3).*w2b(:,3).*rhob(:,3).*(Rb(:,3).^3-Ra(:,3).^3));
m2c3=4/3*pi*(Np(3)*w2c(:,3).*rhoc(:,3).*(Rc(:,3).^3-Rb(:,3).^3));
release3=(m203-(m2a3+m2b3+m2c3))/m203;

m204=4/3*pi*rhoa*w2a0*(Np(4)*(Ra0(4)^3-R0(4)^3));
m2a4=4/3*pi*rhoa*w2a0*(Np(4)*(Ra(:,4).^3-R0(4).^3));
m2b4=4/3*pi*(Np(4).*w2b(:,4).*rhob(:,4).*(Rb(:,4).^3-Ra(:,4).^3));
m2c4=4/3*pi*(Np(4)*w2c(:,4).*rhoc(:,4).*(Rc(:,4).^3-Rb(:,4).^3));
release4=(m204-(m2a4+m2b4+m2c4))/m204;

m205=4/3*pi*rhoa*w2a0*(Np(5)*(Ra0(5)^3-R0(5)^3));
m2a5=4/3*pi*rhoa*w2a0*(Np(5)*(Ra(:,5).^3-R0(5).^3));
m2b5=4/3*pi*(Np(5).*w2b(:,5).*rhob(:,5).*(Rb(:,5).^3-Ra(:,5).^3));
m2c5=4/3*pi*(Np(5)*w2c(:,5).*rhoc(:,5).*(Rc(:,5).^3-Rb(:,5).^3));
release5=(m205-(m2a5+m2b5+m2c5))/m205;

m206=4/3*pi*rhoa*w2a0*(Np(6)*(Ra0(6)^3-R0(6)^3));
m2a6=4/3*pi*rhoa*w2a0*(Np(6)*(Ra(:,6).^3-R0(6).^3));
m2b6=4/3*pi*(Np(6).*w2b(:,6).*rhob(:,6).*(Rb(:,6).^3-Ra(:,6).^3));
m2c6=4/3*pi*(Np(6)*w2c(:,6).*rhoc(:,6).*(Rc(:,6).^3-Rb(:,6).^3));
release6=(m206-(m2a6+m2b6+m2c6))/m206;

m207=4/3*pi*rhoa*w2a0*(Np(7)*(Ra0(7)^3-R0(7)^3));
m2a7=4/3*pi*rhoa*w2a0*(Np(7)*(Ra(:,7).^3-R0(7).^3));
m2b7=4/3*pi*(Np(7).*w2b(:,7).*rhob(:,7).*(Rb(:,7).^3-Ra(:,7).^3));
m2c7=4/3*pi*(Np(7)*w2c(:,7).*rhoc(:,7).*(Rc(:,7).^3-Rb(:,7).^3));
release7=(m207-(m2a7+m2b7+m2c7))/m207;

m208=4/3*pi*rhoa*w2a0*(Np(8)*(Ra0(8)^3-R0(8)^3));
m2a8=4/3*pi*rhoa*w2a0*(Np(8)*(Ra(:,8).^3-R0(8).^3));
m2b8=4/3*pi*(Np(8).*w2b(:,8).*rhob(:,8).*(Rb(:,8).^3-Ra(:,8).^3));
m2c8=4/3*pi*(Np(8)*w2c(:,8).*rhoc(:,8).*(Rc(:,8).^3-Rb(:,8).^3));
release8=(m208-(m2a8+m2b8+m2c8))/m208;

m209=4/3*pi*rhoa*w2a0*(Np(9)*(Ra0(9)^3-R0(9)^3));

```

```

m2a9=4/3*pi*rhoa*w2a0*(Np(9)*(Ra(:,9).^3-R0(9).^3));
m2b9=4/3*pi*(Np(9).*w2b(:,9).*rhob(:,9).*(Rb(:,9).^3-Ra(:,9).^3));
m2c9=4/3*pi*(Np(9).*w2c(:,9).*rhoc(:,9).*(Rc(:,9).^3-Rb(:,9).^3));
release9=(m209-(m2a9+m2b9+m2c9))/m209;

m2010=4/3*pi*rhoa*w2a0*(Np(10)*(Ra0(10)^3-R0(10)^3));
m2a10=4/3*pi*rhoa*w2a0*(Np(10)*(Ra(:,10).^3-R0(10).^3));
m2b10=4/3*pi*(Np(10).*w2b(:,10).*rhob(:,10).*(Rb(:,10).^3-Ra(:,10).^3));
m2c10=4/3*pi*(Np(10).*w2c(:,10).*rhoc(:,10).*(Rc(:,10).^3-Rb(:,10).^3));
release10=(m2010-(m2a10+m2b10+m2c10))/m2010;

%//////////End Release from the ith class//////////

%//////////Figures//////////
figure
plot(t/3600,Ra*10^6,'-',t/3600,Rb*10^6,'--',t/3600,Rc*10^6,'.')
title('Radii evolution')
xlabel('Time [h]')
ylabel('Radius [um]')
legend('Ra','Rb','Rc')

figure
plot(t/3600,w2b,t/3600,w2c)
title('Drug fractions')
xlabel('Time [h]')
ylabel('Mass fraction [-]')
legend('w2b','w2c')

figure
plot(t/3600,release,'-',t/3600,release1,'-',t/3600,release2,'-',t/3600,release3,'-',t/3600,release4,'-',t/3600,release5,'-',t/3600,release6,'-',t/3600,release7,'-',t/3600,release8,'-',t/3600,release9,'-',t/3600,release10,'-')
title('Release from the ith classes')
xlabel('Time [h]')
ylabel('Release [-]')
legend('release TOT','release I','release II','release III','release IV','release V','release VI','release VII','release VIII','release IX','release X')

% %//////////Experimental data//////////

texp=[0.016666667,0.5,1,1.5,2,3,4,5,6,7,9,11,13,15,17,19,21,23,25,27,29,32,33,35,37,39,41,43,45,47,49,51,53,55,57,59,61,63,65,67,69,71,73,75,77];

y20=[1.90240316,6.488009571,10.08250555,14.05554622,18.29947852,25.96874285,33.43354749,40.61199147,47.65716631,54.01040045,66.1672172,75.91891377,82.43046676,87.50249762,91.68557423,92.94562351,96.34256413,92.04639665,98.43055252,100.7490821,99.97138893,100.1995253,101.4802649,99.89193702,98.99139666,100.8077398,100,100,100,100,100,100,100,100,100,100,100,100,100,100,100,100,100,100,100,100,100]; %Global TP release with film thickness of 20 um

y30=[1.310134018,5.100524125,7.501053805,10.1312529,13.43881706,17.69370403,22.73221795,27.66044764,32.35499387,36.98307846,46.18394602,55.09346624,62.83360535,69.7154417,75.46837038,78.27760034,86.41201019,89.42124639,92.19890086,95.74649776,95.51165956,99.26835398,99.19284621,101.168998,99.65818819,99.9796757,100,100,100,100,100,100,100,100,100,100,100,100,100,100,100,100,100,100,100,100,100];

```

```
y60=[1.981569582,5.115953377,6.765312431,8.137103313,9.353900156,11.22879192,
13.79075693,16.71703661,18.902185,21.61699951,26.00686318,30.75278334,35.2802
5299,39.22761513,43.25815544,47.05651527,50.97411896,55.24559284,58.80588289,
62.18060217,65.82993692,68.66016577,71.95850492,74.53939,76.75124643,78.92388
318,82.16850129,84.34895295,85.95549981,87.87383053,89.39914511,90.28398997,9
0.62647986,92.40681804,93.39578489,94.66340375,94.54008634,96.17876151,96.597
20818,97.49118014,97.11047724,97.55955686,98.22587734,99.96597617,98.83363928
]; %Global TP release with film thickness of 60 um
% %////////End Experimental data//////////

figure
plot(texp,y20,'o',texp,y30,'+',texp,y60,'x',t/3600,release*100,'-');
xlabel('Time [h]');
ylabel('Release %');
legend('Exp 20um','Exp 30um','Exp 60um','Mod')

%////////End Figures//////////

end
```